

AMERICAN UNIVERSITY OF BEIRUT

RADIATION-INDUCED DNA DAMAGE IN PODOCYTES:
ROLE OF SMPDL3B IN ATM NUCLEAR SHUTTLING

by
MARINA SIMON FRANCIS

A thesis
submitted in partial fulfillment of the requirements
for the degree of Master of Science
to the Department of Anatomy, Cell Biology, and Physiological Sciences
of the Faculty of Medicine
at the American University of Beirut

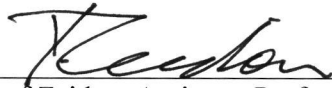
Beirut, Lebanon
September 2019

AMERICAN UNIVERSITY OF BEIRUT

RADIATION-INDUCED DNA DAMAGE IN PODOCYTES: ROLE OF
SMPDL3B IN ATM NUCLEAR SHUTTLING

By

Marina Simon Francis



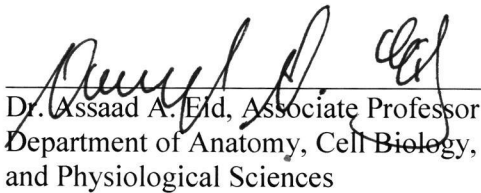
Dr. Youssef Zeidan, Assistant Professor
Department of Radiation Oncology

Advisor



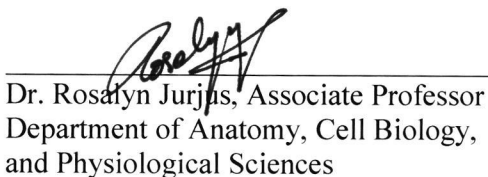
Dr. Alessia Fornoni, Professor
Chief, Katz Family Division of Nephrology and Hypertension
Director, Peggy and Harold Katz Family Drug Discovery Center
Miller School of Medicine, University of Miami

Member of Committee



Dr. Assaad A. Eid, Associate Professor
Department of Anatomy, Cell Biology,
and Physiological Sciences

Member of Committee



Dr. Rosalyn Jurjis, Associate Professor
Department of Anatomy, Cell Biology,
and Physiological Sciences

Member of Committee

Date of thesis defense: September 9, 2019

AMERICAN UNIVERSITY OF BEIRUT

THESIS, DISSERTATION, PROJECT RELEASE FORM

Student name: Francis Marina Simon
Last First Middle

Master's Thesis
Dissertation

Master's Project

Doctoral

I authorize the American University of Beirut to: (a) reproduce hard or electronic copies of my thesis, dissertation, or project; (b) include such copies in the archives and digital repositories of the University; and (c) make freely available such copies to third parties for research or educational purposes.

I authorize the American University of Beirut, to: (a) reproduce hard or electronic copies of it; (b) include such copies in the archives and digital repositories of the University; and (c) make freely available such copies to third parties for research or educational purposes after:

One ---- year from the date of submission of my thesis, dissertation, or project.

Two ---- years from the date of submission of my thesis, dissertation, or project.

Three years from the date of submission of my thesis, dissertation, or project.

Marina
Signature

17-9-19
Date

ACKNOWLEDGMENTS

I would like to extend my heartfelt gratitude to my mentor Dr. Youssef Zeidan for believing in me and for his continuous support throughout this project. His guidance has taught me the ideal research methodology, which rendered me a motivated researcher capable of tackling the challenges in the field.

Many special thanks go to Dr. Assaad Eid, Dr. Larry Bodgi and Dr. Frederic Harb for their help and advice in various aspects of my project.

Additionally, I would like to thank my fellow lab mates for all the lovely moments we spent together during this year. Thank you Alaa and Patrick for helping me develop my research technical skills, and thank you dearest Maya and Sara for always cheering me on and making campus feel so much like home.

Last but not the least, I can't express how grateful I feel towards my family, without whose support I would not have made it this far in my studies.

AN ABSTRACT OF THE THESIS OF

Marina Simon Francis for Master of Science
Major: Physiology

Title: Radiation-Induced DNA Damage in Podocytes: Role of SMPDL3b in ATM Nuclear Shuttling

Background: Radiotherapy (RT) is the primary, non-invasive treatment for over 50% of cancer patients. Despite its curative potential, RT can induce damage in normal healthy tissues surrounding the tumor. The kidneys are radiosensitive organs, hence dose-limiting for RT targeting abdominal and paraspinal tumors. Excessive radiation doses to the kidneys ultimately lead to radiation nephropathy. In fact, podocytes are key players in the pathogenesis of radiation-induced proteinuria. Prior work points to a potential role for the lipid modifying enzyme, SMPDL3b, in regulating the response of podocytes to radiation injury.

Aim: Our current study aims to determine the role of SMPDL3b in DNA double strand breaks (DSBs) repair after radiation injury.

Methods: WT (wild-type) and OE (SMPDL3b overexpressors) immortalized human podocytes were used for this study. Differentiated cultured cells were irradiated and the treatment was stopped at selected time points. γ -H2AX and p-ATM nuclear foci were quantified by confocal microscopy after immunofluorescence (IF) staining. Further investigations on ATM nuclear shuttling were performed on isolated nuclear and cytoplasmic fractions through Western Blotting. Cell survival was assessed by quantifying the protein expression of p-p53 (ser15) and cleaved caspase 3. Furthermore, liquid chromatography – mass spectrometry (LC-MS) analysis was used for the assessment of radiation-induced changes in nuclear sphingolipids in both WT and OE cells. The impact of ceramide-1-phosphate (C1P) or ZOPRA pre-treatments on DSBs recognition and repair through ATM nuclear shuttling was also assessed by IF staining. Viability of irradiated WT and OE podocytes after treatments was assessed by MTT assay.

Results: After assessing the kinetics of γ -H2AX and p-ATM nuclear foci appearance/disappearance in both cell lines, we established that SMPDL3b overexpression in podocytes enhances DSBs recognition and repair by modulating ATM nuclear shuttling. Western Blotting analysis on isolated nuclear and cytoplasmic fractions from both cell lines confirmed enhanced ATM nuclear shuttling in OE podocytes. Moreover, SMPDL3b overexpression protected podocytes from radiation-induced apoptosis by down-regulating the activation of the tumor suppressor protein p53 and subsequent caspase 3 cleavage. The LC-MS results revealed that SMPDL3b overexpression prevented the radiation-induced alterations in nuclear C1P and ceramide levels. Furthermore, the basal levels of nuclear sphingomyelin were significantly lower in OE than in WT podocytes which potentially modulate the fluidity of the nuclear membrane.

Interestingly, exogenous administration of C1P radiosensitized OE by delaying ATM nuclear shuttling and subsequently impairing DSBs recognition and repair. On the other hand, ZOPRA pretreatment radioprotected WT podocytes by accelerating ATM nuclear shuttling and DSBs recognition and repair.

Conclusion: Our results show that SMPDL3b overexpression in podocytes confers radioprotective effects. SMPDL3b plays a key role in the modulation of ATM nuclear shuttling and subsequently DNA damage recognition and repair. This could be potentially explained by changes in the fluidity of the nuclear membrane and nuclear sphingolipids.

CONTENTS

ACKNOWLEDGMENTS	v
ABSTRACT.....	vi
ILLUSTRATIONS	xii
ABBREVIATIONS	xiii
Chapter	
I. INTRODUCTION.....	1
A. Principles of Radiotherapy.....	2
1. Radiotherapy Treatment Planning.....	2
2. Ionizing Radiation-Induced DNA Damage.....	4
a. Direct Effect of Ionizing Radiation:	4
b. Indirect Effect of Ionizing Radiation:	5
c. Types of Ionizing Radiation-Induced DNA Damage:	5
3. Ionizing Radiation Induced DNA Damage Response.....	6
a. Detection of DSBs and Initiation of the DDR:	7
b. Role of ATM in DSBs Repair:	7
c. ATM Nuclear Shuttling:	8
4. Relative Radiosensitivity of Cells and Patients.....	9
a. Differential Radiosensitivity of Cells:	9
b. Differential Radiosensitivity of Patients.....	9
5. Ionizing Radiation-Induced Cell Death and Senescence	11
a. RT-Induced Apoptosis:.....	11
b. RT-Induced Mitotic Catastrophe:	12
c. RT-Induced Necrosis:	12

d. RT-Induced Senescence:.....	13
B. Translational Aspects of Sphingolipids	13
1. Sphingolipids Metabolic Pathway.....	14
2. Role of Sphingolipids in DNA damage response:	15
C. Radiation Induced Nephropathy	18
1. Podocytopathy in Glomerular Diseases	20
2. Role of SMPDL3b in Podocytopathy and Glomerular Diseases:	21
3. Role of SMPDL3b in Radiation Induced Podocytopathy	22
D. Aims and Hypothesis of the Study	23
II. MATERIALS AND METHODS.....	25
A. Human Podocytes Culture	25
B. Exogenous C1P Pretreatment	25
C. ZOPRA Pretreatment.....	26
D. Irradiation.....	26
E. Immunofluorescence Staining	26
F. MTT Assay	27
G. Protein Extraction	28
1. Nuclear and Cytoplasmic Proteins Extraction	28
2. Whole Cell Protein Extraction	28

H.	Western Blotting	29
1.	Nuclear and Cytoplasmic Fractions	29
2.	Whole Cells	29
I.	Liquid Chromatography – Mass Spectrometry (LC-MS) Analysis.....	30
1.	Nuclei Isolation	30
2.	Liquid Chromatography – Mass Spectrometry	31
J.	Statistical Analysis.....	31
III.	RESULTS	31
A.	IR-induced DNA DSBs in human podocytes	31
B.	SMPDL3b overexpression in podocytes enhances DSBs recognition and repair post-IR	33
C.	SMPDL3b overexpression in podocytes accelerates ATM nuclear shuttling post-IR	36
1.	Kinetics of p-ATM Foci Appearance/ Disappearance in WT and OE podocytes.....	36
2.	Effect of SMPDL3b overexpression on ATM Nuclear Shuttling	39
D.	SMPDL3b overexpression in podocytes mitigates the activation of ATM downstream effectors and the induction of apoptosis.....	41
E.	IR induces SMPDL3b re-localization to the nuclear and perinuclear regions ...	43
F.	SMPDL3b overexpression in podocytes prevents IR-induced changes in nuclear sphingolipids.....	44
G.	Exogenous C1P radiosensitizes SMPDL3b overexpressors.....	46

1. Kinetics of γ -H2AX Foci Appearance/ Disappearance in C1P treated and non-treated OE podocytes	46
2. Kinetics of p-ATM Foci Appearance/ Disappearance in C1P treated and non-treated OE podocytes	47
3. Effect of exogenous C1P on SMPDL3b overexpressors viability	49
 H. ZOPRA pre-treatment radioprotects WT podocytes	 51
1. Kinetics of γ -H2AX Foci Appearance/ Disappearance in ZOPRA treated and non-treated WT podocytes	51
2. Kinetics of p-ATM Foci Appearance/ Disappearance in ZOPRA treated and non-treated WT podocytes	52
3. Effect of ZOPRA treatment on WT podocytes viability.....	54
 IV. DISCUSSION	 55
 REFERENCES	 63

ILLUSTRATIONS

Figure	Page
1. Radiation-induced DNA damage.....	4
2. Sphingolipid metabolic pathway.....	15
3. Role of SMPDL3b in radiation-induced podocytopathy.....	23
4. Hypothesis.....	24
5. SMPDL3b overexpression enhances DSBs recognition and repair in podocytes.....	34
6. IR-induced ATM nuclear shuttling.....	36
7. SMPDL3b overexpression in podocytes accelerates ATM nuclear shuttling	38
8. SMPDL3b overexpression enhances ATM nuclear shuttling in podocytes...	40
9. SMPDL3b overexpression mitigates the activation of p53 and subsequent caspase 3 cleavage.....	41
10. IR-induced SMPDL3b relocalization.....	43
11. LC-MS analysis of nuclear sphingolipids post-IR.....	45
12. Exogenous C1P delays DSBs recognition and repair in SMPDL3b overexpressors.....	47
13. Exogenous C1P delays ATM nuclear shuttling in SMPDL3b overexpressors	48
14. Exogenous C1P radiosensitizes SMPDL3b overexpressors.....	49
15. ZOPRA treatment enhances DSBs recognition and repair in WT podocytes	52
16. ZOPRA treatment accelerates ATM nuclear shuttling in WT podocytes.....	53
17. ZOPRA radioprotects WT podocytes.....	54
18. Model of IR-induced DNA damage response in podocytes.....	62

ABBREVIATIONS

ATM: Ataxia telangiectasia mutated

ATR: Ataxia telangiectasia and Rad-3 related

BD: Base damage

Cer: Ceramide

C1P: Ceramide-1-phosphate

CHO: Cholesterol

CKD: Chronic kidney disease

DDR: DNA damage response

DNAPK: DNA-dependent protein kinase

DSB: Double strand break

GFR: Glomerular filtration rate

Gy: Gray (absorbed dose)

HMG-CoA: 3-hydroxy-3-methyl-glutaryl-coenzyme A reductase

HR: Homologous recombination

HSCT: Hematopoietic stem cell transplantation

IR: Ionizing radiation

LC-MS: Liquid chromatography- Mass spectrometry

LET: Linear energy transfer

LPP: Lipid phosphate phosphatases

NHEJ: Non-homologous end joining

NI: Non-irradiated

OE: Overexpressors

PC: Phosphatidylcholine

ROS: Reactive oxygen species

RT: Radiotherapy

RTX: Rituximab

SK: Sphingosine kinase

SM: Sphingomyelin

SMPDL3b: Sphingomyelin phosphodiesterase acid like-3b

S1P: Sphingosine-1-phosphate

SPP: S1P phosphatase

SSB: Single strand break

TBI: Total body irradiation

TSC: Tuberous sclerosis complex

WT: Wild-type

CHAPTER I

INTRODUCTION

Cancer incidence is increasing around the world; it is expected to be the leading cause of death during the 21st century. In 2019, more than 1.7 million cases of cancer are expected to be diagnosed in the USA alone and the death toll from cancer is expected to reach more than 600,000 Americans [1]. This could be attributed to the aging population, detrimental environmental factors, changes in lifestyles caused by socioeconomic advances, as well as hereditary cancer susceptibility [2-4].

More than half of all cancer patients undergo radiotherapy (RT), before or after surgery, or in combination with chemotherapy or immunotherapy. Different treatment regimens are determined based on the location, type, and stage of the tumor [5]. In fact, RT is the primary non-invasive curative treatment for 60% of all cancer patients who are scheduled to receive RT as part of their treatment plan [6].

Soon after Wilhelm C. Röntgen X-rays' discovery in 1895, X-rays were used as a modality to treat tumors and inflammatory diseases. Early side effects and complications were rapidly discovered and taken into consideration. The path for radiotherapy research was paved by introducing the concept of dose fractionation to decrease the burden on the surrounding healthy tissues as well as the concepts of time-dose and dose-volume dependencies. This led to the development of modern and highly precise linear accelerators which allow delivering higher doses to tumors, while preserving normal tissues [7].

A. Principles of Radiotherapy

RT aims at restraining the infinite proliferative capacity of cancerous cells and inducing their death. It is an effective non-invasive modality that limits tumor growth, improves survival and prevents cancer reoccurrence [8, 9].

RT uses ionizing radiation (IR) that deposits energy and forms ions in the targeted cells of the radiated tissue. Eventually, this will either directly kill tumor cells or induce genetic variations leading to their death [5]. Multiple factors affect the success of RT including the radiation sensitivity of targeted cells, linear energy transfer (LET), total delivered dose, and fractionation rate [10, 11].

Ionizing radiation (IR) is delivered to the tumor either externally or internally. Most commonly, an external radiation beam targets the tumor by transmitting external high energy rays including photons of low Linear Energy Transfer (LET) (X-rays and γ -rays) and particle radiation of high LET (α -particles, protons, neutrons, electrons, and heavy ions) [5]. High LET results in increased biological effectiveness and thus proven to be more effective in treating radioresistant tumors such as renal cell carcinoma, glioblastoma, and sarcoma. Unfortunately, the production of particle radiation is more expensive hence favoring the use of photons [12, 13]. Brachytherapy, on the other hand, consists of delivering internal radiation through radioactive sources from inside the body usually on malignant gynecological and prostate tumors [5].

1. Radiotherapy Treatment Planning

RT treatment is planned in a way to reduce the negative impact on the healthy tissues surrounding the targeted tumors. This can be achieved by insuring proper

shielding of healthy tissues and by following an adequate fractionated schedule enabling DNA repair in healthy tissues between sessions. In addition, RT planning ensures that the challenging dose is focused on the tumor while avoiding the surrounding healthy tissues through shaping precisely the radiation beams [14]. For instance, multiple advancements have been done in RT in order to minimize its side effects on the organs at risk while maximizing its curative impact [15]. The modern techniques include 3D conformal RT, intensity modulated RT, volumetric modulated arc therapy, image guided RT, and stereotactic body RT and radiosurgery [7].

The dose fractionation schemes are shaped in order to improve the positive outcomes of RT. Sometimes fractionation plans diverge from the conventional fractionated RT received by most patients, which consists of delivering 1.8 to 2 Gy/fraction, in an effort to enhance its effectiveness [16]. The hypofractionated plan consists of delivering few high doses of 3 to 20 Gy/fraction/day over a short time period. However, the hyperfractionated protocol consists of delivering small fractions without major difference in the duration of the treatment in comparison to conventional RT. Thus, it consists of delivering 0.5 to 2 Gy/fraction twice a day and for a period of 2 to 4 weeks [17]. The concept of dose fractionation helps the surrounding normal tissues to recover due to slower rates of proliferation in comparison to the fast dividing cancerous cells. Consequentially, the latter will accumulate higher amount of DNA damage when they cycle, depending on their radiosensitivity [7].

2. Ionizing Radiation-Induced DNA Damage

High energy radiation results in DNA damage in the targeted cells. Cells lose their ability to further undergo cellular proliferation and eventually die [18]. IR has direct and indirect effects on cellular DNA.

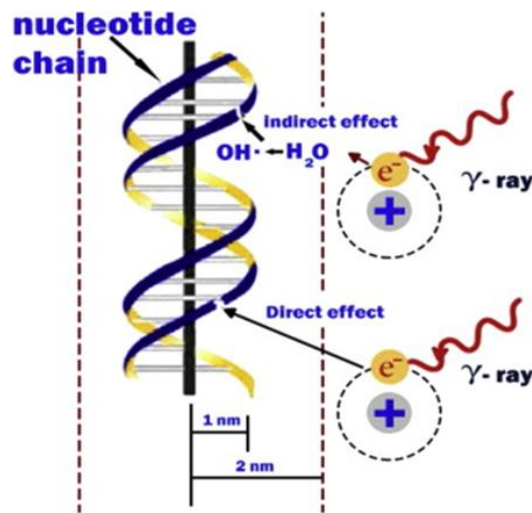


Figure 1: Radiation-Induced DNA Damage. IR induces direct DNA damage through high energy photons and indirect damage through water radiolysis event (Desouky et al. 2015) [19].

a. Direct Effect of Ionizing Radiation:

The direct effect of radiation results when photons, which possess enough energy to knock electrons out of chemical bonds, directly hit DNA molecules. This disrupts their structure either leading to cell death or inducing carcinogenesis if damaged cells survive. This effect prevails with high doses and high LET radiation including α -particles and neutrons [20].

b. Indirect Effect of Ionizing Radiation:

On the other hand, IR induces reactive oxygen species (ROS) production due to water radiolysis, with water being a major constituent of the cell. Actually, this event represents the indirect effect of IR mediated by low LET including X- rays and γ - rays. The generated free radicals and free electrons, that have a very short life span, attack vital macromolecules including nuclear DNA and induce biochemical damage [21, 22]. It's the total dose and not the dose rate that determines the amount of IR-induced ROS. Most IR-induced damage is a consequence of the indirect effects [20].

c. Types of Ionizing Radiation-Induced DNA Damage:

IR-induced DNA damage includes mainly double strands breaks (DSB), single strand breaks (SSB), or base damage:

- Double strand Breaks: DSBs are formed when the chemical bonds of both strands of DNA molecules are broken. Although the number of induced DSBs is relatively low (around 40 DSB/Gy), it is the most difficult form of DNA damage to fix, requiring more than 50 minutes to repair 50% of the damage [23].
- Single strand breaks: SSBs are caused by the cleavage of the phosphodiester bonds in only one strand of the DNA molecule. Thus, both strands remain attached. In fact, 1 Gy can induce around 1000 SSBs, of which 50% get repaired within 10 to 20 minutes post-IR exposure [24, 25].
- Base damage: BD is a common type of DNA damage where a dose of 1 Gy can induce around 3000 BD. These are chemical lesions that mainly include oxidation by ROS, deamination, alkylation as well as hydrolysis leading to serious genomic aberrations [26].

However, DSBs are considered the most lethal forms of IR-induced DNA damage. If unrepaired, DSBs can lead to cell death or genomic rearrangements favoring cancer initiation [20, 26].

3. Ionizing Radiation Induced DNA Damage Response

In response to genomic injuries such as UV, IR, and chemotherapy, cells develop a DNA damage response (DDR). The complex signaling pathways involved in the DDR lead to cell cycle arrest and DNA damage repair, or apoptosis. It serves to maintain genomic integrity of the cells which otherwise if compromised would lead to severe disorders [27].

As mentioned earlier, DSBs are classified as the most lethal forms of IR-induced DNA damage [28]. Since non-homologous end-joining (NHEJ) is the prevailing repair mechanism for DSBs in quiescent mammalian cells, it is thought to be the predominant element of DDR post-RT as most of the human body cells are in quiescence [29]. NHEJ repair is based on the direct ligation of both ends of DSBs, mainly during the G1 phase [30]. However, different NHEJ sub-pathways are thought to co-exist, each of which with a distinct repair half-time [31]. On the other hand, homologous recombination (HR) repair pathway uses genetic information from the homologous chromosomes i.e. from equivalent region found on the second undamaged DNA molecule [30]. This pathway accounts for the systematic repair of only around 15% of IR-induced DSBs [31, 32]. The lethal effect of IR can be well explained by the contribution of unrepaired DSBs due to failure in NHEJ [31].

a. Detection of DSBs and Initiation of the DDR:

The MRN complex, which consists of 3 subunits: Mre11, Nbs1, and Rad50, directly detects DNA damaged sites, mainly DSBs, by binding to the DNA double stranded ends. This complex is responsible of signaling to the DDR upstream kinases including ataxia-telangiectasia mutated protein (ATM) and Rad3-related protein (ATR). In turn, these kinases will activate downstream effectors involved in the DDR signaling pathway in order to modulate the progression of the cell cycle and launch the repair [33]. For instance, ATM and/or ATR activates the tumor suppressor protein p53, which is known to be mutated in most cancers, in order to promote cell cycle arrest and apoptosis [34]. Moreover, ATM and ATR activate the checkpoint kinases (CHK1 and CHK2) which can either stimulate apoptosis and cell cycle arrest through p53 activation [35] or independently by activating BRCA2. The latter initiates a repair process [36].

b. Role of ATM in DSBs Repair:

Members of the phosphatidylinositol-3 kinases family, including ATM, ATR and DNA-dependent protein kinase (DNAPK), are responsible for the phosphorylation of the histone variant H2AX (at Ser 139) near DSBs. In effect, γ -H2AX (phosphorylated H2AX) formation is a very early step in the DDR of mammalian cells. It plays an essential role in recruiting damage signaling factors to DSBs sites essential for repair induction [37, 38]. In their experiments, Burma et al. demonstrated that nuclear γ -H2AX foci formation after DNA damage induction was severely reduced in ATM^{-/-} fibroblasts but normal in DNAPK^{-/-} fibroblasts. In addition, the administration of a DNAPK inhibitor (wortmannin) in ATM^{-/-} cells abolished completely γ -H2AX foci formation. These results show that ATM is the primary kinase responsible for the rapid

phosphorylation of H2AX in response to DNA DSBs and that DNAPK, rather than ATR, takes this job in the absence of ATM [39]. However, ATR is the kinase involved in the phosphorylation of H2AX in response to DNA SSBs and replicative stress [40, 41].

c. ATM Nuclear Shuttling:

Strong evidence suggests that IR triggers the monomerization of cytoplasmic ATM dimers through oxidation reactions, resulting in p-ATM (phosphorylated ATM) monomers with increased kinase activity [32, 42]. ATM monomers then bind to importins through their nuclear localization signals (NLS) and are subsequently shuttled into the nucleus [43, 44]. This phenomenon is proportionate to the delivered dose [32]. Once inside the nucleus, p-ATM will be guided to DSBs sites by signals from the MRN complex. p-ATM will phosphorylate the 3 subunits of the MRN complex as well as the histone variant H2AX resulting in formation of nuclear foci. This will ensure DSBs recognition and the initiation of the repair [44-46]. p-ATM nuclear shuttling and foci formation at DSBs is a very rapid process. The maximal number of nuclear p-ATM foci is usually reached within 10min to 1hr post-IR [47].

However, certain cytoplasmic proteins like mutated huntingtin or tuberous sclerosis complex (TSC) can bind activated ATM monomers and impede their shuttling towards the nucleus. This results in delayed p-ATM shuttling and impaired DSBs recognition and repair, thus increasing radiosensitivity [46, 48].

4. Relative Radiosensitivity of Cells and Patients

Strong evidence suggests that radiosensitivity is highly variable among different cell types and patients. This could potentially explain the various degrees of RT adverse effects ranging from non-significant or mild to severe.

a. Differential Radiosensitivity of Cells:

The law of Bergonie and Tribondeau states that progenitor cells that undergo active cell division are highly radiosensitive in contrast to differentiated cells. The progenitor cells may either be replaced by new ones if killed by radiation or induce secondary cancers if they survive with unrepaired DNA. Radiosensitivity results in the loss of replicative abilities of progenitor cells or loss of cell function in differentiated cells. In addition, radiosensitivity varies according to the nucleus size. It increases in cell types with large nuclei because the nuclear contents, mainly DNA and DNA associated-nuclear membranes, are the most radiosensitive cellular elements [20, 21].

b. Differential Radiosensitivity of Patients

Around 5 to 15% of RT patients develop tissue overreaction leading to change in treatment plan and increased morbidity [49, 50]. Radiosensitivity is dose-dependent and is molecularly based on unrepaired DNA DSBs [51]. Eventually, unrepaired DSB will result in unrepaired chromosome breaks and micronuclei formation [52].

Radiosensitivity is associated with syndromes resulting from mutations of proteins involved in DSBs repair or mutations of cytoplasmic proteins like huntingtin and tuberous sclerosis complex [46, 53, 54]. In fact, the most radiosensitive syndromes are ataxia telangiectasia (AT) and Ligase IV (Lig4). AT is an autosomal recessive disease caused by mutations in ATM kinase which is an essential protein in mediating DSBs

repair through the phosphorylation of the histone variant H2AX [55-59]. Ligase IV syndrome is caused by mutations in LIG4 gene which is an important component of nonhomologous end-joining repair (NHEJ) of DSBs in mammals [59].

According to Granzotto, Benadjaoud et al. (2016), the maximum number of nuclear ATM foci in skin fibroblasts at early time points, that is 10min and 1hr post-irradiation, and the number of nuclear γ -H2AX foci at 24hrs post-irradiation allow the classification of patients into four groups:

- Group I patients: Radioresistant and have a low risk of cancer due to fast ATM nuclear shuttling which results in complete DSBs recognition and then repair.
- Group II patients: moderately radiosensitive and have high risk of cancer due to delayed ATM nuclear shuttling and weakened DSBs recognition.
- Group IIIa patients: hyper-radiosensitive and have a very high risk of cancer due to mutations of ATM leading to massive failure of DSBs recognition and repair.
- Group IIIb patients: hyper-radiosensitive and have a very high risk of cancer due to mutations of Ligase IV leading to massive failure of DSBs repair.

Pereira, Bodgi et al. developed a fast ELISA-based assay to predict clinical radiosensitivity. This assay, which has the highest statistical performance among other predictive tests, aims at quantitating nuclear active forms of ATM monomers after isolation of nuclear and cytoplasmic fractions. The data obtained were in accordance with nuclear ATM foci quantification and stresses that an individual's radiosensitivity could be predicted, with some accuracy, based on the radiation-induced ATM nuclear shuttling theory [47].

5. Ionizing Radiation-Induced Cell Death and Senescence

RT aims at depriving cancerous cells from their reproductive capabilities when treating tumors, mainly by inducing apoptosis. Strong evidence suggests that the therapeutic outcome of RT doesn't rely on apoptosis alone but rather involves various cell death mechanisms such as mitotic catastrophe, necrosis, and senescence. The tumor suppressor gene, p53, is a key player in these cellular responses [8]. Cancer cell death doesn't occur instantaneously, and can take up to weeks from treatment cessation [5].

During tumor progression, pro-apoptotic mechanisms are lost mainly due to impaired functional p53 in more than 50% of human malignant tumors [60-62]. The radiation-activated p53 signals cell cycle arrest and DNA damage repair, thus promoting cell survival. On the other hand, it can also stimulate the elimination of injured cells through apoptosis or senescence depending on the cell type and the extent of the DNA damage [63]. However, tumors may resist apoptosis by retaining functional p53 due to pro-apoptotic genes deactivation (Bax, Apaf1...) or elevated expression of anti-apoptotic genes (Bcl2, survivin...) [64].

a. RT-Induced Apoptosis:

After irradiation, multiple proteins involved in the death receptor pathway, that might be dependent or independent of p53, are up-regulated and lead to IR- induced apoptosis [65]. As a matter of fact, there's an association between radiation-induced apoptosis and the activation of the ATM/ p53/ Bax/ Cytochrome C/ Caspases pathway [66]. A positive correlation exists between the amount of IR- induced apoptosis and the tumor response although apoptosis might not be the primary form of cell death in solid tumors [67].

b. RT-Induced Mitotic Catastrophe:

Mitotic catastrophe designates cell death occurring during or as a consequence of abnormal mitosis [68]. This will result in aberrant segregation of chromosomes leading to the generation of huge cells that either possess an abnormal nuclear morphology, are multinucleated [69-72], and/or have multiple micronuclei [73]. It has been suggested that the mitotic catastrophe occurs as a result of defective cell cycle checkpoints or due to DNA damage that mostly affects p53 leading to its mutation and inactivation [8, 74]. It can be also caused by p53-dependent centrosomes proliferation which results from damaged DNA and defective repair [75-79]. In fact, the delayed cell death induction by RT in solid tumors is mainly caused by the mitotic catastrophe [8] associated with p53/ Cytochrome c/ Caspases pathway [80].

c. RT-Induced Necrosis:

In contrast to apoptosis, necrosis is an uncontrolled cell death which is characterized by various morphological changes including increased cell volume and swelling of organelles, ruptured plasma membranes, and loss of intracellular components. However, as is the case with apoptosis, it is regulated by several catabolic and signal transduction pathways involving TNF α / PARP/ JNK/ Caspases [81, 82]. Necrosis is a form of death that involves immunological activation and pro-inflammatory responses through the release of damage- associated molecular patterns including high mobility group (box1) and heat shock proteins (HSPs) [83, 84]. Mitotic catastrophe is usually followed by necrosis, which is why local inflammation develops post-RT [85].

d. RT-Induced Senescence:

Senescence is a condition of permanent cell cycle arrest which mediates radiation-induced inhibition of tumor growth [8]. It's clinically proven in prostate cancers and desmoids tumors post-RT as a major mechanism for tumor regression [86-88]. Senescent cells preserve their metabolic activity and viability. They are flattened, enlarged cells with a granular cytoplasm. They are rich in vacuoles which can be detected by various biomarkers through histo-chemical staining techniques [8, 89].

A DNA damage response (DDR) develops after low doses of radiation in order to sense the damage and amplify the transmitted signaling cascade. This activates cell cycle arrest, transiently, allowing for DNA damage repair. However, persisting unrepaired damage triggers cell death through p-53 dependent apoptosis, p53-independent mitotic catastrophe, or senescence [90]. Chronic DDR signaling and senescence hinder damage propagation to the next generation of cells [91].

B. Translational Aspects of Sphingolipids

Sphingolipids are no longer thought to be only major structural components of biological membranes but have recently proven to be, along with their active metabolites (ceramide, sphingosine, sphingosine-1-phosphate, ceramide-1-phosphate...), key players in various human diseases [92]. These bioactive signaling molecules mediate various important biological processes such as cell growth, survival, senescence and death [93].

Sphingolipids are a class of lipids characterized by a sphingosine backbone, an amino-alcohol compound with 18 carbon atoms, synthesized from non-sphingolipid

precursors in the endoplasmic reticulum (ER). The diversity of sphingolipids arises from distinct variations of this basic structure [94].

1. Sphingolipids Metabolic Pathway

Ceramide (Cer) is the central metabolite generated within sphingolipid metabolism through 3 different pathways:

- Cer de novo synthesis: Palmitoyl- CoA is condensed with serine by the action of serine palmitoyl transferase followed by a set of reduction and acetylation reactions to generate ceramide.
- Sphingomyelin (SM) catabolism: SM is catabolized by sphingomyelinases, and ceramide is produced.
- Salvage pathway: N-acylation of fatty acids bound to a sphingosine backbone through the action of ceramide synthases, produces ceramide [27].

Cer can be phosphorylated by ceramide kinase into ceramide-1-phosphate (C1P) in trans-Golgi or plasma membranes. C1P plays an important role in inflammatory responses and in cell survival and proliferation [92, 94]. Afterwards, C1P can be dephosphorylated by C1P phosphatases or other unspecific lipid phosphate phosphatases (LPP family) [94, 95]. On the other hand, Cer can be catabolized by ceramidases into sphingosine which promotes cell cycle arrest and apoptosis. In its turn, sphingosine can be phosphorylated by sphingosine kinases into the pro-survival sphingosine-1-phosphate (S1P) [93]. Furthermore, S1P can be dephosphorylated by S1P phosphatases [96, 97] or unspecific LPP [98], generating sphingosine which can be further used to produce Cer or S1P [97]. S1P lyase is considered as the last enzyme in

the sphingolipid catabolic pathway because it can irreversibly breaks down S1P into phosphoethanolamine and hexadecenal [99].

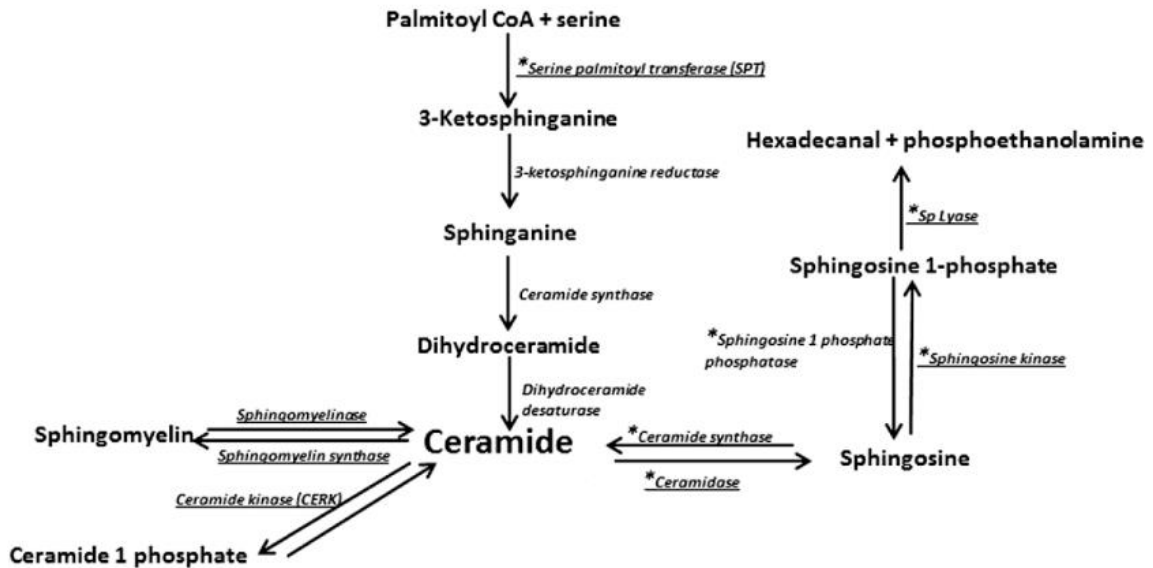


Figure 2: Sphingolipid Metabolic Pathway. Ceramide is the central metabolite generated in the sphingolipid metabolism by three distinct pathways (adapted from Obanda et al. 2015) [100].

2. Role of Sphingolipids in DNA damage response:

Various chemotherapeutic drugs and DNA damaging agents target sphingolipid metabolizing enzymes. Strong evidence suggests that lipids are involved in DNA damage response (DDR) and determining cells fate [27]. Most of cancer treatments lead to ceramide generation, which is implicated in cell death response [101]. However, cancer cells tend to develop survival strategies like generating the pro-survival sphingolipid metabolite S1P after the phosphorylation of sphingosine generated by ceramide hydrolysis [102]. In fact, regulation of the production of these metabolites is

of significant importance in determining the cells' fate in response to DNA damage [27].

According to Dbaibo et al. (1998), p53 is involved in ceramide-induced apoptosis. The accumulation of ceramide in Molt4 lymphocyte leukemia cells post-irradiation and actinomycin D is p53-dependent since increased p53 precedes ceramide up-regulation. Indeed, ceramide accumulation can be impeded by p53 inhibition [103]. p53 is a downstream effector activated by ATM in DDR and numerous evidence implicates its involvement in ceramide accumulation. Prior work demonstrated that IR can't induce apoptosis in AT cells with a mutated ATM gene. These cells maintain the first phase of ceramide accumulation by acid sphingomyelinase but lose the second peak [104]. ATM thus mediates ceramide synthase activation but not the activation of acid sphingomyelinase. Further studies point at the involvement of neutral sphingomyelinases 2 and 3 in DDR where ATM and p53 activates neutral sphingomyelinase 2 and down-regulate neutral sphingomyelinase 3 in order to induce apoptosis [105, 106].

It has been shown that IR induces caspase 3 and PARP cleavage through ceramides. In DDR, ceramide up-regulation is upstream from caspase-3 cleavage. Caspase-3 inhibition doesn't affect the levels of ceramides whereas ceramide depletion prevents the cleavage of caspase-3 and PARP [104, 107] .

Ceramides have been implicated in cell cycle arrest during DDR. For instance, accumulation of ceramides can arrest the cell cycle either at G0/G1 phase mediated by the retinoblastoma protein (Rb) [108] or at G2 phase through the activation of p21 [109]. Moreover, ATM and p53 also play a role in cell cycle arrest during DDR [110].

Remarkably, the mechanisms involved in ceramide-induced apoptosis can be affected by beclin-2 (bcl-2), which regulates cell death [107], whereas those of ceramide-induced cell cycle arrest are bcl-2 independent [109].

The levels of the pro-survival bioactive lipid S1P are also involved in DDR and the determination of cell fate [27]. A link between p53 and sphingosine kinase 1 (SK1), which produce S1P, was established after treating Molt-4 leukemia cells with multiple chemotherapeutic agents and γ -rays. This was followed by a decrease in the protein but not mRNA levels of SK1, associated with p53 up-regulation during DDR [111]. Also, sphingosine kinase 2 (SK2) was shown to exacerbate the apoptotic response and its overexpression is associated with the induction of apoptosis. In addition, SK2 has proved critical for p21 expression needed for cell cycle arrest in a p53-independent route [112, 113].

On the other hand, S1P phosphatase 1 (SPP1) knockdown had a protective role against DNA damage and cell death induced by daunorubicin in MCF7 cells [114]. Expression of SPP1 and SPP2 was shown to be greatly reduced in human colorectal cancers in comparison to healthy adjacent tissues [115]. Furthermore, according to Oskouian et al. (2006), augmenting S1P lyase activity through its overexpression or by treatment with etoposide, a topoisomerase II inhibitor, favors apoptosis through caspase-3, annexin-V, and PARP as well as nuclear condensation .

Taken together, these findings reveal the importance of sphingolipids in mediating the DNA damage response.

C. Radiation Induced Nephropathy

Radiation nephropathy is IR-induced renal injury that occurs after irradiating both kidneys with a sufficient single dose or multiple fractionated ones [116]. The first case of radiation-induced nephropathy was published in 1927 [117]. In fact, the kidneys are dose-limiting organs for RT owing to their central location in the abdomen and their high radiosensitivity. This is especially the case when treating tumors in the abdominal and paraspinal regions, or during total body irradiation (TBI) administered prior to hematopoietic stem cell transplantation (HSCT) [118, 119]. It has been reported that 10% to 30% of HSCT patients will eventually suffer from chronic kidney disease (CKD) [120].

The threshold dose for the induction of radiation nephropathy has been set at 23 Gy, fractionated into 20 small doses, after irradiating both kidneys over 4 weeks [121]. Also, radiation nephropathy may occur within a year post a single dose of 10 Gy for TBI or due to fractionated dose of 14 Gy over 3 days [122]. It's worth noting, however, that irradiation which targets less than 30% of total kidney volume will not cause CKD but the injury may be sufficient to induce hypertension [123].

Radiation nephropathy will develop in less than 50% of patients subjected to threshold or even higher IR doses depending on the individual's radiosensitivity [14]. Renal injury usually takes months to years to manifest after IR exposure because renal tissues have slow cell turnover and mitotic rates [124].

The kidneys are vital organs that filter electrolytes and metabolic wastes from circulating blood, modulate blood pressure through the electrolytes-fluid balance, and also produce erythropoietin which is needed for the stimulation of red blood cells production in the bone marrow [118]. Therefore, radiation nephropathy has various

clinical manifestations depending on the radiation dose and volume [118, 125]. TBI-induced renal failure leads to thrombocytopenia and microangiopathic hemolytic anemia among other systemic complications, with a clinical presentation similar to that of hemolytic uremic syndrome [126].

Acute and sub-acute radiation nephropathy develops within 3 to 18 months after exposure and results in decreased glomerular filtration rate (GFR) and increased serum levels of β_2 -microglobulin [127, 128]. Other symptoms include fatigue, edema, azotemia, malignant hypertension, mild proteinuria and severe anemia [121, 124, 129-131].

Chronic radiation nephropathy manifests in a similar manner to renal failure. It leads to proteinuria, albuminuria and edema, hypertension, azotemia, anemia, and kidney atrophy. It could either be primary following irradiation with first presentation up to 2 years or more, or secondary. The latter develops in patients who had suffered from the acute phase then present with the manifestations of CKD progressing towards end stage renal disease. Consequentially, these patients will require either hemodialysis or kidney transplant [121, 132], both of which are associated with high rates of morbidity and mortality.

On the histological level, kidney irradiation causes changes that can be classified as early and late side-effects. The early changes consist of endothelial cell swelling and microvascular injury, expansion of the subendothelial space with accumulation of amorphous material and mesangiolytic tubular injury. The late changes however consist of glomerular scarring and fibrosis, mesangial expansion with residual damage of the parenchyma, sclerosis of the arcuate and interlobular arteries and atrophy of the renal tubules resulting in decreased renal mass [119, 133].

Moreover, radiation might influence tissue repair pathways which manifests as a late damage to normal tissues by inducing non-lethal cellular changes. Subsequent alteration in the cellular microenvironment follow, consisting of up-regulated chemokines, fibrotic and inflammatory cytokines, disrupted cell to cell interactions, and influx of inflammatory cells [134].

1. Podocytopathy in Glomerular Diseases

It has been demonstrated previously that the glomerulus is primarily targeted in IR-induced kidney damage [135]. The highly specialized and terminally differentiated podocytes are key players involved in the development of proteinuria in glomerular diseases including diabetic nephropathy and focal segmental glomerulosclerosis [132]. The appropriate function of podocytes requires the maintenance of their actin cytoskeleton integrity [136]. Multiple studies emphasized the important role of sphingolipids in maintaining normal podocytes function [137-139].

Differentiated renal podocytes are always in a post-mitotic state, meaning that they don't display active proliferation. Podocytes possess distinctive shape and location essential for basic glomerular filtration [140]. The foot processes of adjacent podocytes interdigitate and interact with the glomerular basement membrane forming the slit diaphragms, while their large cell bodies bend into the capsule's Bowman space. These slits are essential for proper filtration allowing only the passage of small molecules from the blood into the first urinary ultra-filtrate [139].

The integrity of the podocytes maintains the proper functioning of the glomerular filtration barrier. Multiple stressors lead to podocytes injury resulting in

functional abnormalities. These include ionizing radiation, genetic mutations, malignancies, metabolic stress, inflammatory responses and hemodynamic changes [141]. The filtration barrier becomes compromised due to structural changes induced by cytoskeletal remodeling of podocytes that dysregulate the foot processes. In fact, foot processes widening and loss allow large molecules that usually don't cross into the filtrate to pass. This includes the negatively charged proteins leading to proteinuria, which is a distinctive mark of glomerular diseases [142].

2. Role of SMPDL3b in Podocytopathy and Glomerular Diseases:

Multiple studies emphasize the important role of sphingolipids in maintaining normal podocyte function and their implication in genetic and non-genetic glomerular diseases [137-139]. The specific expression of sphingomyelin phosphodiesterase acid-like 3b (SMPDL3b) in podocytes was reported to be a modulator of the activity of acid sphingomyelinase and stress signaling. SMPDL3b intrinsic enzymatic activity still needs to be fully elucidated. However, it has been shown that SMPDL3b resides in the lipid rafts of podocytes plasma membrane and participates in ceramide production by sphingomyelin hydrolysis. Strong evidence suggests that SMPDL3b is critical for preserving podocytes proper functioning [143]. A novel work pinpointed that SMPDL3b regulates C1P levels in podocytes by either inhibiting ceramide kinases activity or dephosphorylating C1P [144]. SMPDL3b expression was reduced in podocytes of patients with FSGS and was associated with altered sphingomyelinase activity and podocytes actin cytoskeleton remodeling. Consequently, cell migration and proteinuria develop [139]. However, SMPDL3b deficiency can be reversed by administering rituximab (RTX), an anti-CD20, which was demonstrated to bind

SMPDL3b [145]. Furthermore, Tasaki, Shimizu et al. (2014) demonstrated that, RTX impedes proteinuria after kidney transplantation in baboons and precipitates SMPDL3b in the glomeruli of pigs [146]. On the other hand, the elevated expression of SMPDL3b is associated with diabetic nephropathy [139]. Hence, it can be inferred that modulation of SMPDL3b, albeit in different manners, is involved in multiple glomerular diseases through compromising the normal functioning of podocytes

3. Role of SMPDL3b in Radiation Induced Podocytopathy

In order to determine the role of SMPDL3b in IR-induced podocytopathy, Ahmad et al. (2016) conducted a study on wild-type (WT) and SMPDL3b overexpressors (OE) podocytes. They demonstrated that a single radiation dose of 8 Gy results in a time-dependent drop in protein levels of SMPDL3b, and in levels of sphingosine and S1P in WT podocytes. On the other hand, the levels of various pro-apoptotic ceramide species were significantly elevated including these of C16:00, C24:00 and C24:1 species. Furthermore, podocytes showed loss of filopodia and cortical actin remodeling starting at 2hrs post-irradiation. This is caused by the relocalization of ezrin, an actin binding protein at the plasma membrane, into the cytosol [132].

In contrast, SMPDL3b OE podocytes displayed increased basal levels of S1P and were protected against the radiation-induced ceramides up-regulation and cytoskeletal remodeling. OE also revealed enhanced DNA damage repair evidenced by reduced γ -H2AX nuclear foci formation by one third in comparison to WT at 2hrs post-IR. Interestingly, RTX treatment before irradiation partially protected WT podocytes

from SMPDL3b protein loss, filopodia effacement, and caspase-3 mediated apoptosis [132].

These results imply that SMPDL3b overexpression and RTX pretreatment *in vitro* protect podocytes from the devastating effects of radiation. Therefore, SMPDL3b plays a major role in IR-induced podocytopathy [132].

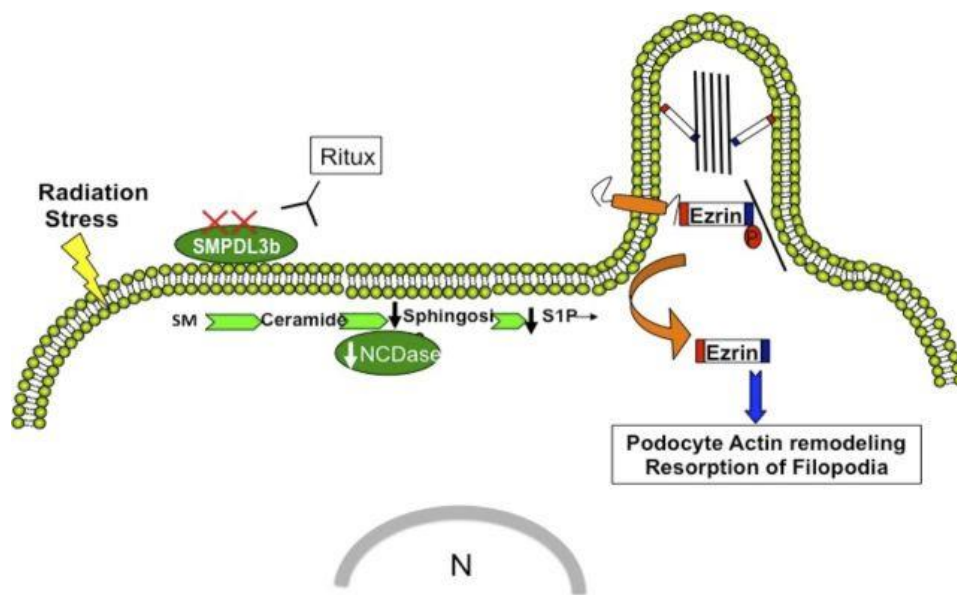


Figure 3: Role of SMPDL3b in Radiation-Induced Podocytopathy. Radiation-induced SMPDL3b down-regulation results in changes in sphingolipid metabolism and actin cytoskeleton remodeling. NCDase: neutral ceramidase, Ritux: rituximab anti-CD20, SMPDL3b: sphingomyelin phosphodiesterase acid-like 3b, SM: sphingomyelin, S1P: sphingosine-1-phosphate (Ahmad et al. 2016) [132].

D. Aims and Hypothesis of the Study

Kidneys are highly radiosensitive organs that perform vital physiological functions and are hence dose-limiting for RT that targets nearby tumors. Therefore,

developing pharmacological interventions that can protect patients from the lethal effects of radiation-induced nephropathy is clinically valuable.

Our current study aims to unravel the SMPDL3b-mediated molecular pathways involved in radiation-induced DDR in human podocytes. We also aim to identify new potential pharmacological agents targeting the sphingolipid metabolism to mitigate radiation-induced renal damage in oncology patients.

We hypothesize that the lipid modifying enzyme, SMPDL3b, plays a critical role in DNA damage repair through the modulation of ATM nuclear shuttling.

This could be potentially explained by changes in the nuclear membrane fluidity which is currently under investigation. Furthermore, we hypothesize that radiation-induced SMPDL3b down-regulation leads to changes in nuclear sphingolipid metabolites which might be also implicated in the DDR.

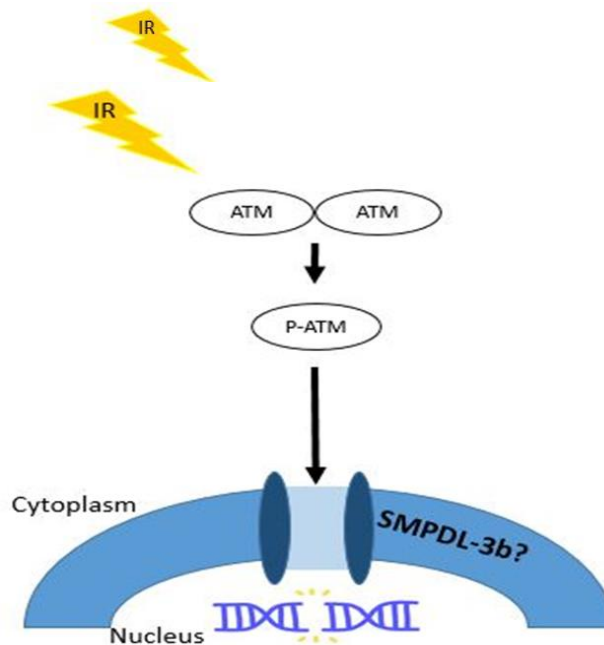


Figure 4: Hypothesis: The lipid modifying enzyme, SMPDL3b, plays a critical role in DNA damage repair through the modulation of ATM nuclear shuttling.

CHAPTER II

MATERIALS AND METHODS

A. Human Podocytes Culture

Immortalized human podocytes: wild-type (WT) and SMPDL3b overexpressors (OE) were cultured in RPMI 1640 medium (Sigma-Aldrich, Steinheim, Germany) supplemented by 10% FBS (Sigma-Aldrich), 1% penicillin/streptomycin (Biowest) and 0.2% plasmocin prophylactic (InvivoGen ant-mpp, San Diego, USA). Cells were seeded on collagen coated (CELL Applications) 100mm dishes or cover-glasses placed in 24-well plates. Podocytes were incubated at 33°C to proliferate and 1% of 100x insulin-transferrin-selenium (Gibco, USA) was added to the medium until the cells reached 70% confluency. Afterwards, they were left to differentiate at 37°C for 10-14 days.

B. Exogenous C1P Pretreatment

Exogenous C1P pretreatment was administered as described previously [143]. C1P stock solution (Echelon Biosciences) was prepared by dissolving C1P in autoclaved nanopure water and subjecting it to sonication at 4°C to ensure a clear dispersion. Differentiated cells were incubated at 37°C for 1hr in a medium containing 30µM C1P before irradiation.

C. ZOPRA Pretreatment

ZOPRA pretreatment was administered as described previously [46, 48].

Differentiated cells were incubated at 37°C for 24hrs in a medium containing 1µM pravastatin (Sigma-Aldrich) dissolved in PBS. Afterwards, the medium was discarded and replaced by a medium containing 1µM zoledronate (Sigma-Aldrich) in PBS and the cells were incubated at 37°C for 12hrs. After that, the medium was changed prior to irradiation.

D. Irradiation

Irradiation was delivered as a single dose of 2Gy from an X-RAD 225 KV precision X-ray irradiator PXI (North Branford, CT) according to the manufacturer's recommendations. The dose rate was set at 285 cGy/min.

E. Immunofluorescence Staining

WT and OE Podocytes were cultured and differentiated at 37°C on collagen-coated coverglasses placed in 24-well plates. Cells were fixed with 4% paraformaldehyde for 20 min at room temperature and permeabilized with a cold lysis solution containing 0.5% Triton X-100 for 7 min at room temperature. Afterwards, cells were incubated with either p-ATM (Anti-phospho-ATM (Ser1981), Merck, Millipore), γ -H2AX (Anti-phospho-Histone H2AX (Ser139), Merck, Millipore) or SMPDL3b (Genway) primary antibodies with a dilution of 1:150 in 3% bovine serum albumin-phosphate buffered saline (BSA-PBS) for 1hr 30min at 37°C. Fluorescence was detected by using Alexa fluor 488 anti-mouse or anti-rabbit secondary antibodies

(Thermo-Fisher Scientific) that were added to the cells and incubated for 30 min at 37°C with a dilution of 1:150 in 3% BSA-PBS. DAPI stained fluoroshield (Abcam) drops were placed on the slide on which the cover-glasses were mounted. A laser scanning confocal microscope (Zeiss LSM 710) was used to examine the slides and to collect the images. To quantify p-ATM and γ -H2AX nuclear foci, 90 nuclei were assessed for each time point. Each 30 nuclei belonged to an independent experiment.

F. MTT Assay

An MTT assay kit was purchased from Abcam and the procedure was applied as per the manufacturer's recommendation. Briefly, WT and OE cells were seeded at 15000 cells/well on collagen-coated 24-well plates and incubated for 24hrs at 33°C. Afterwards, cells were shifted for differentiation at 37°C and C1P or ZOPRA pretreatment was administered as described earlier before irradiation. The MTT assay was applied at 24hrs post-irradiation. The cultured medium was discarded and replaced with a serum-free medium. The MTT reagent was then added and the cells were incubated for 3hrs at 37°C. Then, the MTT solvent was added and the plates were placed on an orbital shaker for 15min. The solution of each condition was re-suspended properly and transferred to a 96 well-plate in order to measure the absorbance at 590nm using a microplate reader (Multiskan EX, Thermo-Fisher Scientific). The percentages of radiation-induced cytotoxicity in OE podocytes with or without C1P, or in WT podocytes with or without ZOPRA pretreatment were calculated for 3 independent experiments.

G. Protein Extraction

Nuclear, cytoplasmic, and whole cell proteins were extracted in order to be analyzed by western blotting. The concentrations of the proteins were determined by Bio-rad Lowry assay (Bio-Rad, Hercules, CA).

1. Nuclear and Cytoplasmic Proteins Extraction

Nuclear and cytoplasmic fractions isolation was performed as described previously [32]. Cell pellets were incubated for 10 min at 4°C in a cytoplasmic buffer (10 mM HEPES pH 7.9, 10 mM KCl, 1.5 mM MgCl₂, 0.5 mM DTT, 2 mM EDTA pH 8, 0.2% Nonidet NP40, protease and phosphatase inhibitors). Cytoplasmic fractions were collected as the supernatants after centrifuging the samples at 2000g for 10 min at 4°C. Afterwards, the remaining pellets were incubated for 1hr at 4°C in a nuclear buffer (20mM HEPES pH 7.9, 450 mM KCl, 1.5 mM MgCl₂, 2 mM EGTA pH 8, 2 mM EDTA pH 8, 0.5 mM DTT, 25% glycerol, protease and phosphatase inhibitors). The supernatants that contained the nuclear fractions were collected after centrifuging the samples at 10000g for 10 min at 4°C.

2. Whole Cell Protein Extraction

Human podocytes were lysed by scraping the 100mm dishes using cold RIPA buffer (150 mM NaCl, 1% NP-40, 0.5% sodium deoxycholate, 0.1% Sodium dodecyl sulfate, and 50 mM Tris pH 8). Samples were subjected to sonication (DIAGENODE Bioruptor) of 10 cycles (30s/cycle). Then, purified proteins were collected as the supernatant after a centrifugation at 13500 rpm, for 30 min at 4°C.

H. Western Blotting

1. Nuclear and Cytoplasmic Fractions

For immunoblotting, 5 µg of nuclear proteins and 25 µg of cytoplasmic proteins were separated on a 6% polyacrylamide gel Electrophoresis (Bio-Rad Laboratory, CA, USA) and transferred overnight at 30V, at 4°C to nitrocellulose membranes (Bio-Rad Laboratory, CA, USA). The blots were blocked with 5% BSA in Tris buffered saline-tween (TBST) for 1 hr. Afterwards, the blots were incubated overnight at 4°C with mouse monoclonal anti-phospho ATM (Ser1981) antibody (1:1000, Merck, Millipore), mouse monoclonal anti-ATM antibody (1:1000, Thermo-Fisher Scientific), rabbit polyclonal anti-topoisomerase II α antibody (1:1000, Cell signaling Technology) and mouse polyclonal anti- α -tubulin (1:800, Abcam). The primary antibodies were detected using anti-rabbit or anti-mouse horseradish peroxidase-conjugated IgG (1:10000, Bio-Rad). Bands were visualized by enhanced chemiluminescence (Bio-Rad) after exposure to X-ray films (Carestream) and developed by the X-omat machine (Carestream). Densitometry analysis was performed using ImageJ software.

2. Whole Cells

For immunoblotting, 40 µg of proteins were separated on 12 or 15% polyacrylamide gel Electrophoresis (Bio-Rad Laboratory, CA, USA) and transferred for 2hrs on ice at 300 mA to nitrocellulose membranes (Bio-Rad Laboratory, CA, USA). The blots were blocked with 5% BSA in TBST for 1 hr. Afterwards, the blots were incubated overnight at 4°C with rabbit polyclonal anti-phospho p53 (ser15) antibody

(1:1000, Cell Signaling Technology), rabbit polyclonal anti-p53 antibody (1:1000, Cell Signaling Technology), rabbit polyclonal anti-active and pro-caspase 3 antibody (1:500, Abcam) and mouse polyclonal anti-GAPDH (1:1000, Santa Cruz). The primary antibodies were detected using anti-rabbit or anti-mouse horseradish peroxidase–conjugated IgG (1:10000, Bio-Rad). Bands were visualized by enhanced chemiluminescence (Bio-Rad) after exposure to X-ray films (Carestream) and developed by the X-omat machine (Carestream). Densitometry analysis was performed using ImageJ software.

I. Liquid Chromatography – Mass Spectrometry (LC-MS) Analysis

Changes in nuclear sphingolipids post-irradiation were analyzed by LC-MS after podocytes' nuclei isolation.

1. Nuclei Isolation

Cells are removed by gentle scraping from their dishes and washed twice with cold PBS. Afterwards, cells are resuspended in 1ml/million cells of cold nuclei isolation buffer containing 320mM sucrose, 10mM HEPES, 5mM MgCl₂, and 1% Triton X-100 at pH of 7.4. Then, cells are vortexed for 10 sec and incubated on ice for 10 min. Nuclei were pelleted after a centrifugation at 2000g and washed twice with nuclei washing buffer having the same composition as the nuclear isolation buffer except Triton X-100.

2. *Liquid Chromatography – Mass Spectrometry*

Nuclear pellets containing 2×10^6 nuclei per sample were subjected to liquid extraction. LC-MS analysis of nuclear sphingolipids was performed at the Medical University of South Carolina using electrospray ionization/tandem MS as previously described [147].

J. **Statistical Analysis**

Results are expressed as means \pm SEM. One-way or two-way ANOVA were used to compare groups. The results were considered statistically significant if $p < 0.05$ (Graph Pad Prism software; La jolla, CA, USA).

Immunofluorescence data were fitted according to Bodgi's formula which describes the kinetics of nuclear foci appearance and disappearance induced by the re-localization of certain proteins caused by genotoxic stress [44]. Kaleidagraph v.4 (Synergy Software, Reading, PA, USA) was used for statistical analysis.

$$N(t) = ID \left(1 - \frac{1}{1 + (b_{rec} \times t)} \right)^{a_{rec}} \left(\frac{1}{1 + b_{rep} (t - t_0)} \right)^{a_{rep}}$$

$N(t)$: number of nuclear foci at a post-irradiation time t

I : number of foci induced/ Gy

D : dose (Gy)

a_{rec} and b_{rec} : recognition rate parameters

a_{rep} and b_{rep} : repair rate parameters

t_0 : delay between recognition and repair processes

CHAPTER III

RESULTS

A. IR-induced DNA DSBs in human podocytes

Previous studies have demonstrated that the number of IR-induced DSBs is linearly dose (D)-dependent along with the induction rate (I_{DSB}). It is considered as a spontaneous event at biological time scale [148, 149]. We were first interested in determining the number of IR-induced DSBs ($N_{\text{DSB}}(t=0s, D=1\text{Gy})$) in human podocytes. This number is affected by the amount of nuclear DNA and by the deposited energy density capable of inducing at least 1 DSB. The number of IR-induced DSBs is given by: $N_{\text{DSB}}(t, D) = I_{\text{DSB}} \times D$ [32]. By fitting our experimental data to the equation, we established that in human podocytes, X-rays radiation induces around (56 ± 2) DSBs per 1Gy.

B. SMPDL3b overexpression in podocytes enhances DSBs recognition and repair post-IR

The earliest step of NHEJ-mediated DSBs recognition is the phosphorylation of H2AX and the formation of nuclear γ -H2AX foci [39, 42, 148, 150]. However, residual γ -H2AX foci, that persist after a long time post-irradiation (post-IR), are considered as recognized but unreparable damage [151]. Previously, our group showed that SMPDL3b OE podocytes have reduced γ -H2AX foci compared to WT at 2hrs post-IR [132]. Accordingly, we wanted to assess the effect of SMPDL3b overexpression on the kinetics of γ -H2AX foci appearance/ disappearance in non-irradiated (NI) and irradiated WT and OE cells (Fig. 5B). We found that an OE cell has, on average, a number of spontaneous nuclear γ -H2AX foci (1.7 ± 0.7) similar to WT (2.3 ± 0.9). However, OE cells scored, on average, a significantly higher number of γ -H2AX foci/ cell (94 ± 4) than WT cells (77 ± 3 , $p < 0.05$) at 10min post-IR (Fig. 5C). In addition, OE cells displayed on average a significantly lower number of residual γ -H2AX foci/ cell (6 ± 1.7) at 24hrs post-IR when compared to WT cells (12 ± 0.3 , $p < 0.05$) (Fig. 5D). Altogether, these results suggest that SMPDL3b overexpression enhances DSBs recognition (at 10min) and repair (at 24hrs).

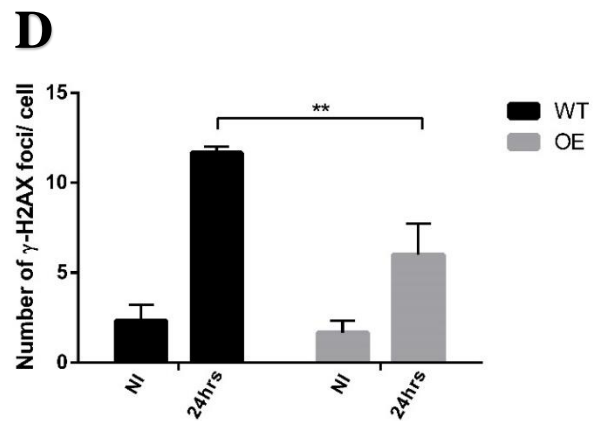
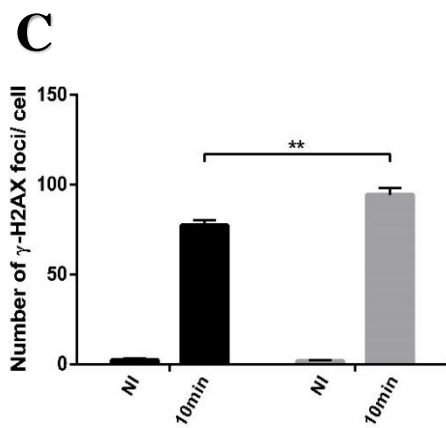
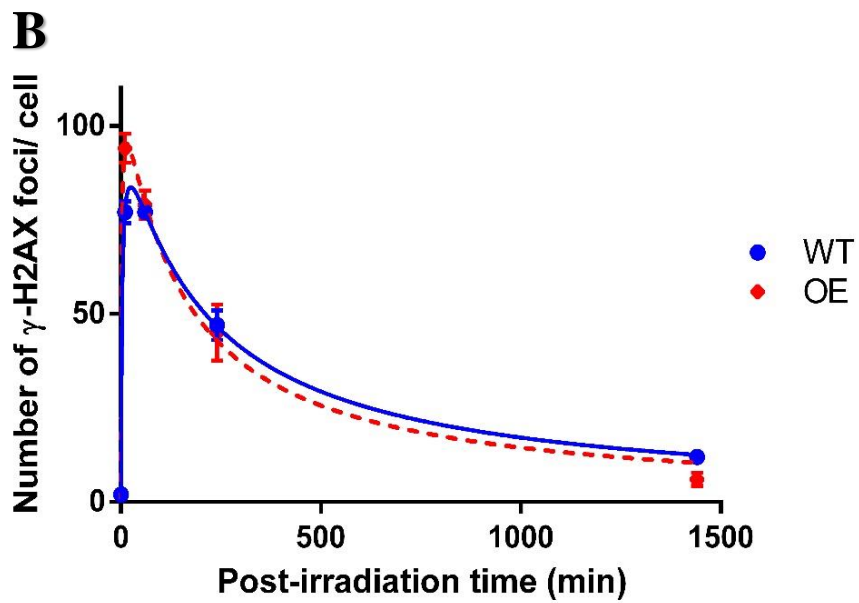
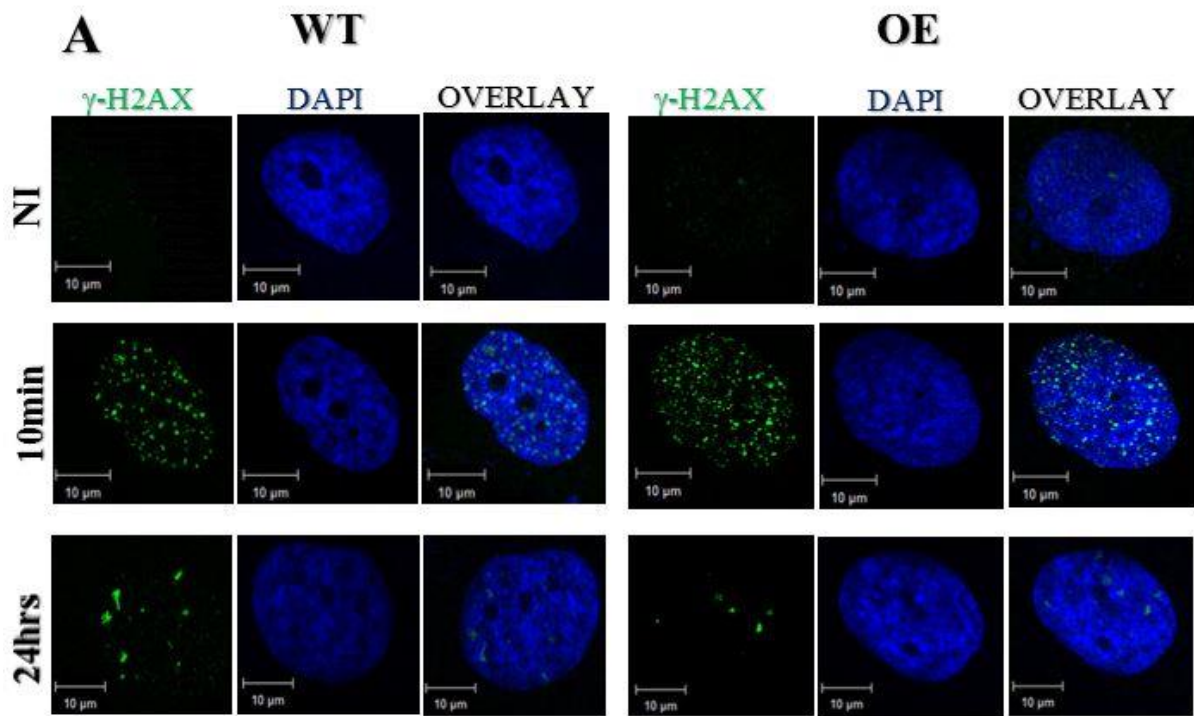


Figure 5: SMPDL3b overexpression enhances DSBs recognition and repair in podocytes. Immunofluorescence staining for γ -H2AX was applied for WT and OE podocytes which were exposed to 2Gy X-rays. (A) Representative laser scanning confocal images of γ -H2AX and DAPI stained nuclei of non-irradiated (NI) and irradiated (10min and 24hrs post-IR) WT and OE podocytes. Magnification $\times 100$. (B) The numbers of γ -H2AX foci in both cell lines were plotted against post-irradiation times. Each plot represents the mean \pm SEM of 3 independent experiments. (C) and (D) The numbers of γ -H2AX foci assessed at 0, 10min and 24hrs post-IR in panels (A) and (B) are reported in histograms.

C. SMPDL3b overexpression in podocytes accelerates ATM nuclear shuttling post-IR

IR triggers the monomerization of cytoplasmic ATM dimers by auto-phosphorylation [32, 42] and subsequent nuclear shuttling [32, 43, 44, 51, 152, 153]. In order to confirm ATM shuttling in podocytes, we stained for p-ATM monomers in NI and irradiated WT cells. We clearly noticed that p-ATM is mainly localized in the cytoplasm of NI cells (Fig. 6A). However, following irradiation, we detected mainly p-ATM nuclear foci at the sites of DSBs with decreased cytoplasmic intensity (Fig. 6B). Therefore, these results confirm IR-induced ATM nuclear shuttling in podocytes.

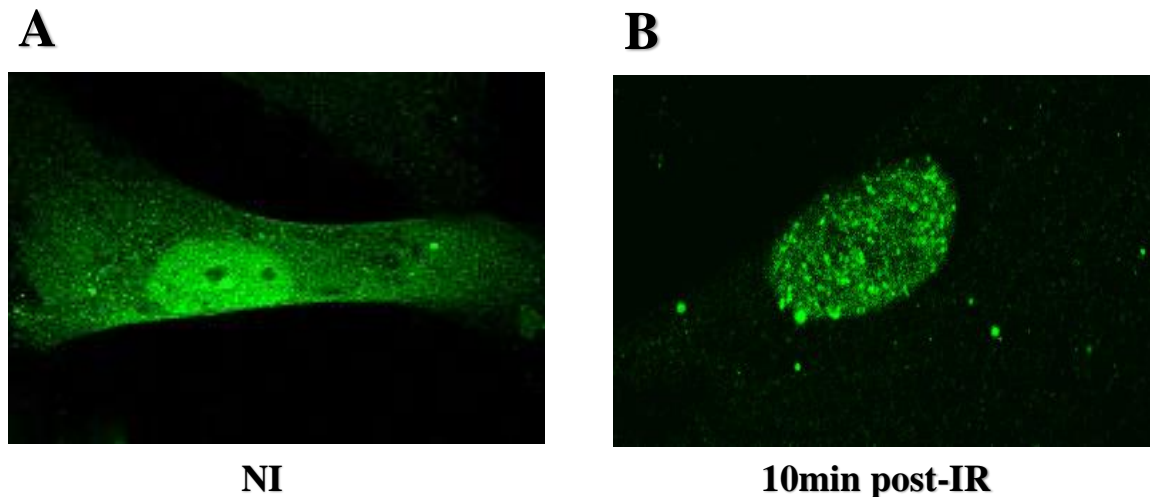


Figure 6: IR-induced ATM nuclear shuttling. Representative laser scanning confocal images of immunofluorescence staining for p-ATM: (A) non-irradiated (NI) and (B) irradiated (10min post-IR) podocytes. Magnification $\times 100$.

1. Kinetics of p-ATM Foci Appearance/ Disappearance in WT and OE podocytes

ATM is the primary kinase responsible for the rapid phosphorylation of H2AX in response to DNA DSBs [39]. We were next interested in investigating whether SMPDL3b overexpression affects the kinetics of γ -H2AX foci through the modulation of ATM nuclear shuttling. Thus, we assessed the kinetics of p-ATM foci in NI and

irradiated WT and OE cells at 10min, 1hr, 4hrs, and 24hrs post-IR (Fig. 7B). We found that an OE cell has on average a number of spontaneous nuclear p-ATM foci (2.0 ± 0.6) similar to WT (1.7 ± 0.3). However, OE cells scored, on average, a significantly higher number of p-ATM foci/ cell (88 ± 1) than WT cells (77 ± 2 , $p<0.01$) at 10min post-IR (Fig. 7C). Both cell lines scored their maximal number of p-ATM foci at 10min post-irradiation. Therefore, these results suggest that SMPDL3b overexpression accelerates ATM nuclear shuttling and kinase activity in response to IR.

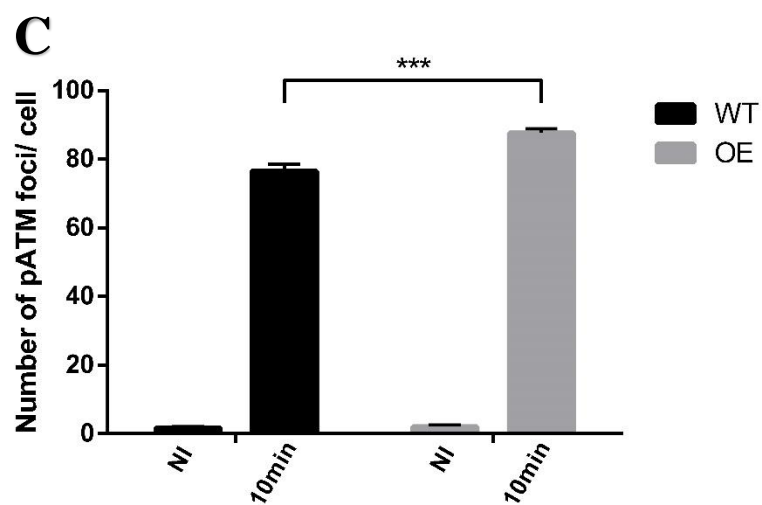
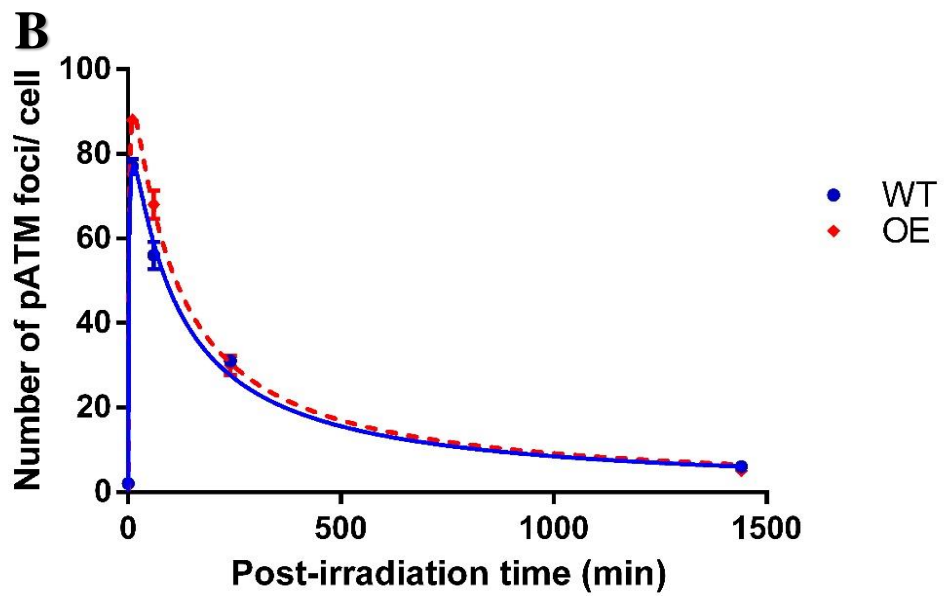
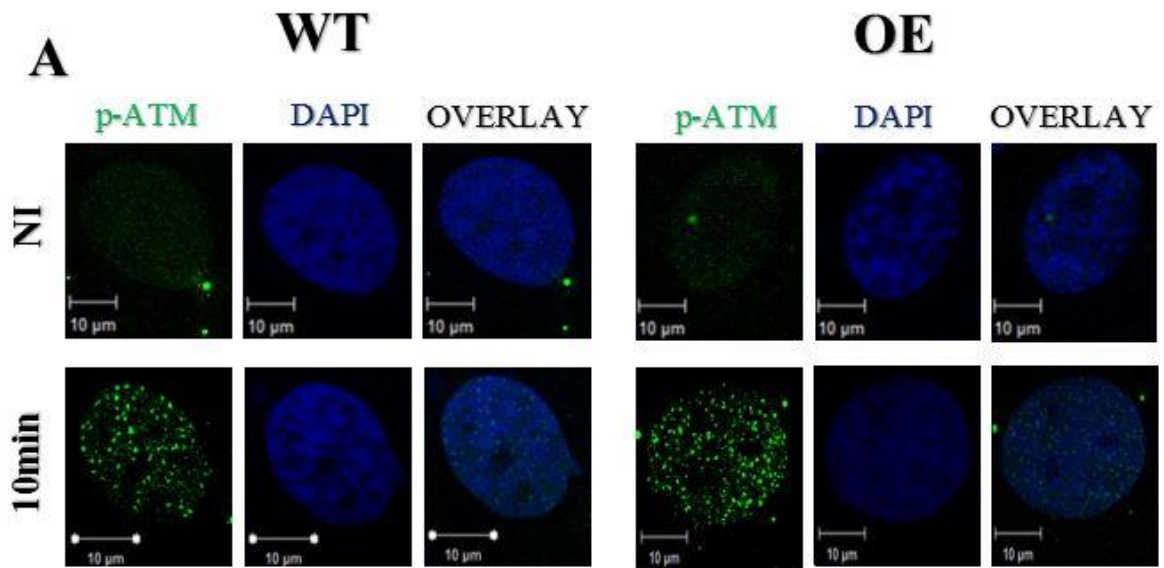


Figure 7: SMPDL3b overexpression in podocytes accelerates ATM nuclear shuttling. Immunofluorescence staining for p-ATM was applied for WT and OE podocytes which were exposed to 2Gy X-rays. (A) Representative laser scanning confocal images of p-ATM and DAPI stained nuclei of non-irradiated (NI) and irradiated (10min post-IR) WT and OE podocytes. Magnification $\times 100$. (B) The numbers of p-ATM foci in both cell lines were plotted against post-irradiation times. Each plot represents the mean \pm SEM of 3 independent experiments. (C) The numbers of p-ATM foci assessed at 0 and 10min post-irradiation in panels (A) and (B) are reported in histograms.

2. Effect of SMPDL3b overexpression on ATM Nuclear Shuttling

To confirm our previous results, we performed nuclear-cytoplasmic fractions isolation on both OE and WT podocytes. The effect of SMPDL3b overexpression on ATM nuclear shuttling was examined through western blot analysis on fractions from both cell lines. Both pATM monomers and ATM dimers were assessed (Fig. 8). We detected significant quantities of p-ATM and ATM proteins basally and post-IR in the nuclear fractions of OE but not in WT. In contrast, p-ATM was significantly detected in the cytoplasmic fractions of WT but was negligible in OE. Significant quantities of ATM dimers were detected in the cytoplasmic fractions of both cell lines. These results support our previous data that SMPDL3b overexpression enhances ATM nuclear shuttling in podocytes.

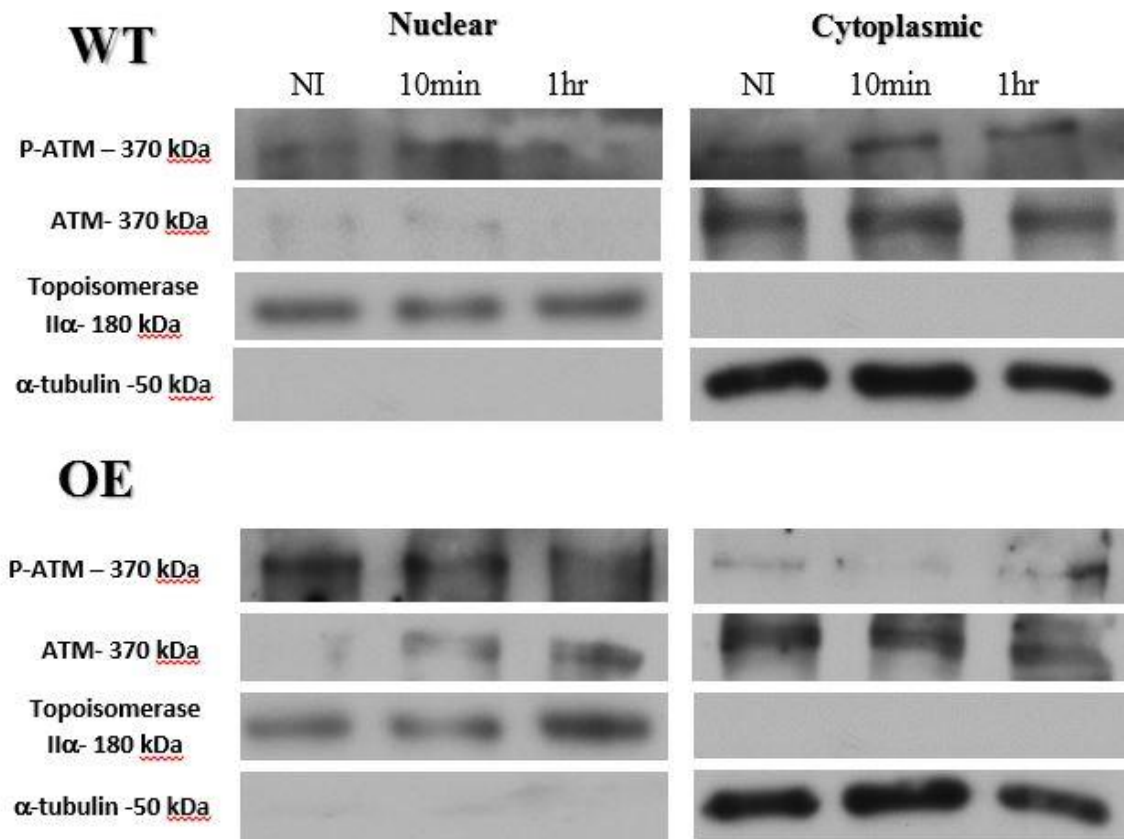


Figure 8: SMPDL3b overexpression enhances ATM nuclear shuttling in podocytes. Representative western blots of p-ATM and ATM from nuclear (5 μ g) and cytoplasmic (25 μ g) extracts of non-irradiated (NI) and irradiated WT and OE podocytes (10min and 1hr post-IR). Topoisomerase and α -tubulin were considered as nuclear and cytoplasmic loading controls respectively.

D. SMPDL3b overexpression in podocytes mitigates the activation of ATM downstream effectors and the induction of apoptosis

ATM can activate the tumor suppressor protein p53 to promote cell cycle arrest and apoptosis [34, 35]. Therefore, we were interested in investigating whether SMPDL3b overexpression affects signaling downstream of ATM. Through western blot analysis, we detected decreased protein levels of p-p53 (Fig. 9A) and cleaved caspase 3 (Fig. 9B) in OE compared to WT mainly at 2hrs post-IR. These results suggest that SMPDL3b overexpression protects podocytes from IR-induced cell death potentially by promoting efficient DSBs repair.

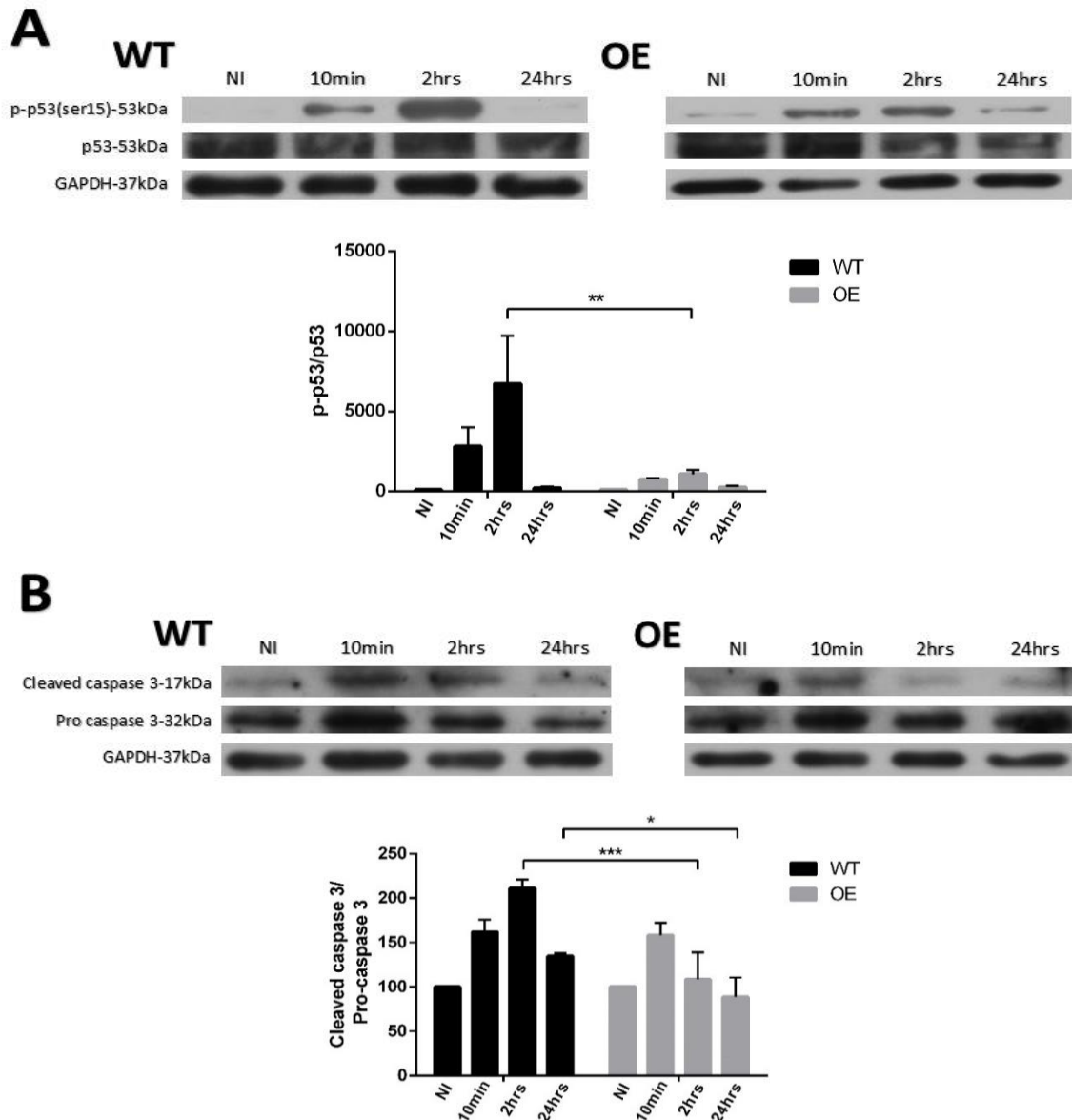


Figure 9: SMPDL3b overexpression mitigates the activation of p53 and subsequent caspase 3 cleavage. Cells were seeded on 100mm dishes and pellets were collected from non-irradiated and irradiated (10min, 2hrs, 24hrs post-IR) OE and WT podocytes. (A) Phosphorylated p53 (p-p53ser15) and (B) cleaved caspase 3 protein expressions were assessed in both cell lines through western blot. Results were quantified by densitometry using Image J software, normalized to total p53 in (A) and to pro-caspase 3 in (B) and expressed as percentage of the non-irradiated control.

E. IR induces SMPDL3b re-localization to the nuclear and perinuclear region

It has been shown previously that SMPDL3b resides in the lipid rafts of the podocytes' plasma membrane [143]. We aimed next for detecting the effect of IR on SMPDL3b localization and expression. We stained for SMPDL3b in NI and irradiated WT podocytes (5min, 10min, 1hr, 4hrs, and 24hrs post-IR) (Fig. 10). We clearly noticed that SMPDL3b is mainly located on the plasma membrane in NI cells. Following irradiation, we detected gradual translocation of SMPDL3b to the nucleus starting at 5min post-IR. However, the intensity of stained SMPDL3b starts to decrease at 4hrs post-IR confirming the previous results [132]. Therefore, IR modulates SMPDL3b localization and expression.

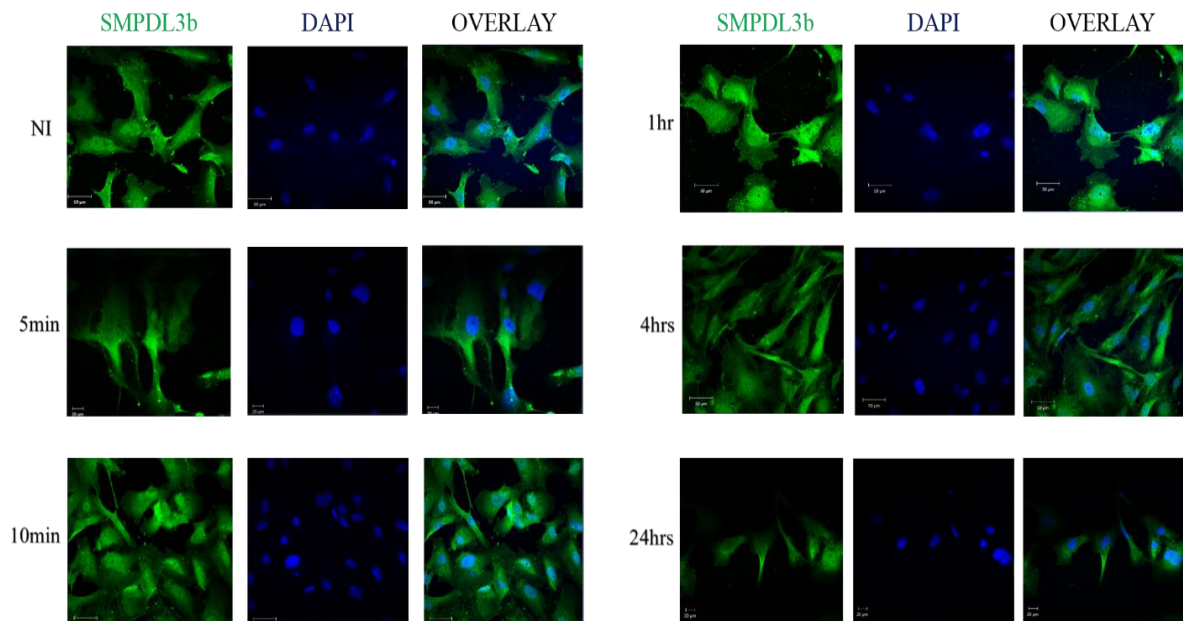


Figure 10: IR-induced SMPDL3b re-localization. Representative laser scanning confocal images of immunofluorescence staining for SMPDL3b (green) and DAPI staining for nuclei (blue) in non-irradiated (NI) and irradiated (5min, 10min, 1hr, 4hrs, 24hrs post-IR) WT podocytes. Magnification $\times 40$.

F. SMPDL3b overexpression in podocytes prevents IR-induced changes in nuclear sphingolipids

Our group has shown previously that SMPDL3b OE podocytes displayed increased basal levels of S1P and were protected against the radiation-induced ceramides up-regulation [132]. Moreover, our collaborators have recently demonstrated that SMPDL3b overexpression down-regulates C1P levels in podocytes [144]. Therefore, we aimed to check for the levels of nuclear sphingolipids post-IR in WT and OE podocytes. NI and irradiated WT and OE podocytes were subjected to nuclei isolation followed by nuclear lipids extraction. Mass spectrometry (MS) analysis in WT podocytes revealed 2 phases of nuclear C1P up-regulation at 5min ($p<0.0001$) and 6hrs ($p<0.01$) post-IR (Fig. 11A). On the other hand, these results were coupled to 2 phases of nuclear ceramides down-regulation at 5min ($p<0.0001$) and 6hrs ($p<0.0001$) (Fig. 11B). Conversely, SMPDL3b overexpressors displayed significantly decreased basal levels of nuclear C1P and ceramides compared to WT which did not get affected by irradiation (Fig. 11A-B). Nuclear sphingomyelin and sphingosine levels did not significantly change post-IR in both cell lines (Fig. 11C-D). However, the basal and post-IR levels of sphingomyelin in WT podocytes were significantly higher than those in SMPDL3b overexpressors ($p=0.0001$) (Fig. 10C). Nuclear S1P levels were below detection levels in both cell lines.

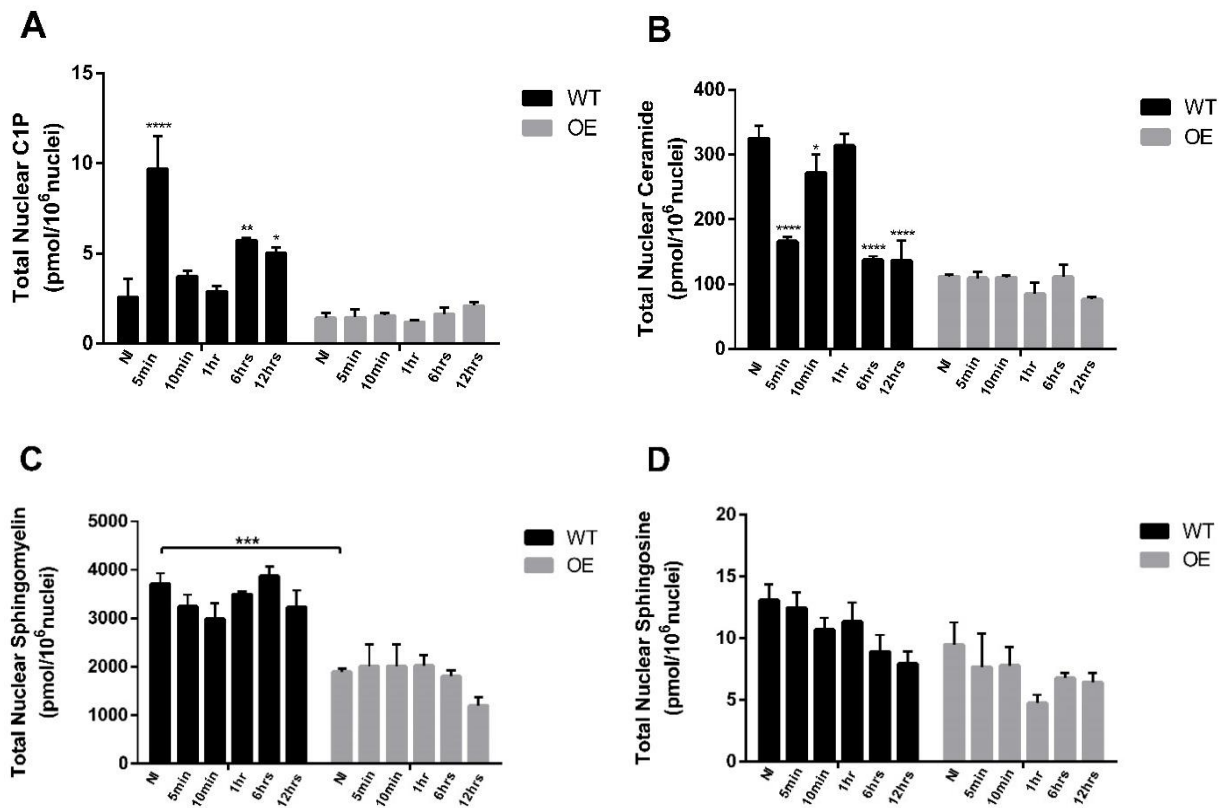


Figure 11: LC-MS analysis of nuclear sphingolipids post-IR. Non-irradiated (NI) and irradiated (5min, 10min, 1hr, 6hrs, and 12hrs post-IR) with a single dose of 2Gy, OE and WT podocytes were subjected to nuclei isolation. Pellets containing 2×10^6 nuclei were collected. Bligh Dyer extraction of lipids was applied and the different groups were subjected to MS analysis to determine the levels of (A) nuclear C1P, (B) nuclear ceramide, (C) nuclear sphingomyelin, and (D) nuclear sphingosine. Results are represented as means \pm SEM from 3 independent experiments ($*p < 0.05$).

G. Exogenous C1P radiosensitizes SMPDL3b overexpressors

The LC-MS results showed that SMPDL3b overexpressors maintain the reduced basal levels of nuclear C1P post-IR conversely to WT cells. We next assessed the effect of C1P pre-treatment on DSBs recognition and repair through ATM nuclear shuttling in SMPDL3b overexpressors.

1. Kinetics of γ -H2AX Foci Appearance/ Disappearance in C1P treated and non-treated OE podocytes

We assessed the kinetics of DSBs recognition and repair by quantifying γ -H2AX foci in NI and irradiated OE cells, with or without C1P pre-treatment, at 10min, 1hr, 4hrs and 24hrs post-irradiation (Fig. 12A). We found that a treated OE cell has, on average, a number of spontaneous nuclear γ -H2AX foci (1 ± 0) similar to a non-treated cell (1.7 ± 0.7). However, treated OE cells scored, on average, a significantly lower number of γ -H2AX foci/ cell (75 ± 1) than non-treated cells (94 ± 4 , $p=0.0001$) at 10min post-IR (Fig. 12B). In addition, treated OE cells displayed on average a significantly higher number of residual γ -H2AX foci/ cell (10 ± 0) at 24hrs post-IR compared to non-treated cells (6 ± 1.7 , $p<0.05$) (Fig. 12C). Altogether, these results suggest that C1P potentially modulates DSBs recognition and repair.

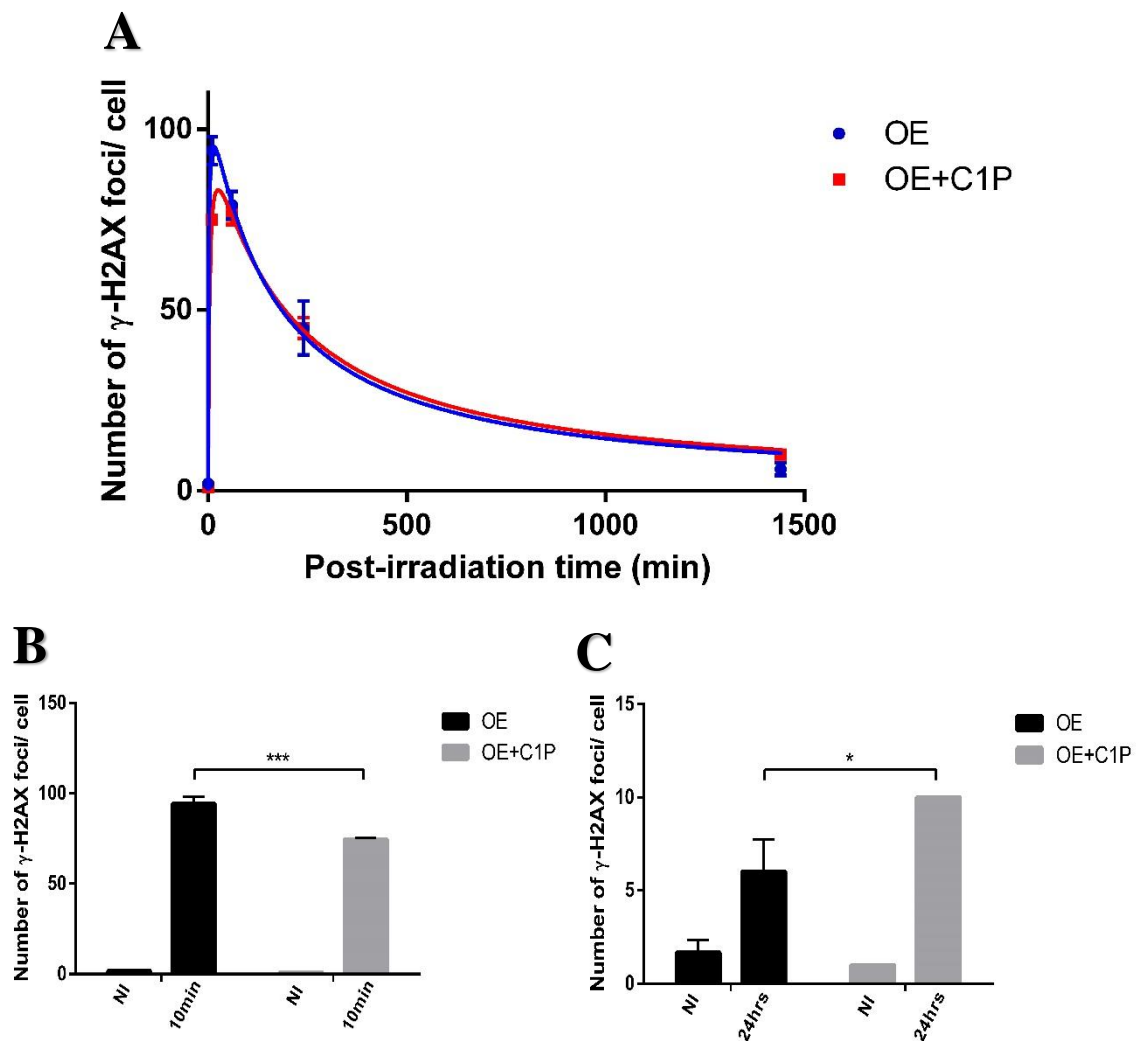


Figure 12: Exogenous C1P delays DSBs recognition and repair in SMPDL3b overexpressors. Immunofluorescence staining for γ -H2AX was applied for C1P treated and non-treated OE podocytes which were exposed to 2Gy X-rays. (A) The numbers of γ -H2AX foci in both groups were plotted against post-irradiation times. Each plot represents the mean \pm SEM of 3 independent experiments. (B) and (C) The numbers of γ -H2AX foci assessed at 0, 10min and 24hrs post-IR in panels (A) are reported in histograms.

2. Kinetics of p-ATM Foci Appearance/ Disappearance in C1P treated and non-treated OE podocytes

In order to check whether elevated nuclear C1P modulates ATM nuclear shuttling, we assessed the kinetics of p-ATM foci in NI and irradiated OE cells, with or

without C1P pre-treatment, at 10min, 1hr, 4hrs, and 24hrs post-IR (Fig. 13A). We found that a treated OE cell has on average a number of spontaneous nuclear p-ATM foci (3.3 ± 0.3) similar to a non-treated cell (2.0 ± 0.6). However, treated OE cells scored, on average, a significantly lower number of p-ATM foci/ cell (57 ± 2) than non-treated cells (88 ± 1 , $p < 0.0001$) at 10min post-irradiation (Fig. 13B). Both groups scored their maximal number of p-ATM foci at 10min post-irradiation. These results suggest that C1P potentially regulates ATM nuclear shuttling in response to IR.

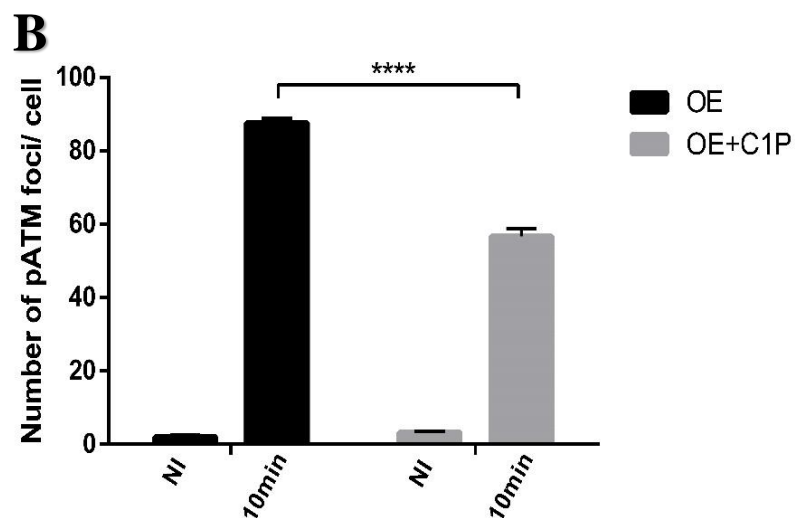
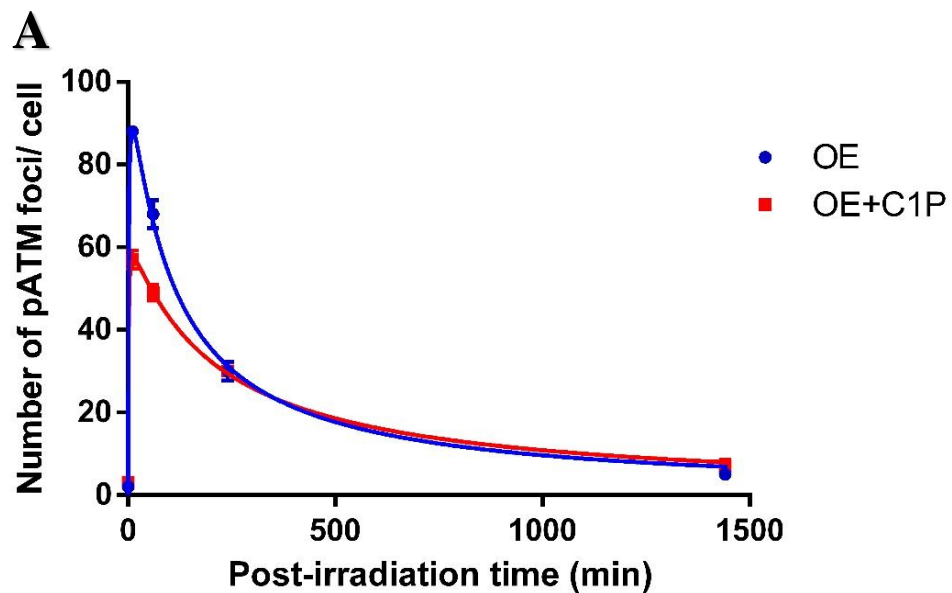


Figure 13: Exogenous C1P delays ATM nuclear shuttling in SMPDL3b overexpressors. Immunofluorescence staining for p-ATM was applied for C1P treated and non-treated OE podocytes which were exposed to 2Gy X-rays. (A) The numbers of p-ATM foci in both groups were plotted against post-irradiation times. Each plot represents the mean \pm SEM of 3 independent experiments. (B) The numbers of p-ATM foci assessed at 0 and 10min post-irradiation in panels (A) are reported in histograms.

3. Effect of exogenous C1P on SMPDL3b overexpressors viability

As the exogenous administration of C1P to OE podocytes resulted in impaired DSBs repair and ATM shuttling, we were next interested in assessing its effect on cell viability with or without irradiation. For this purpose, cytotoxicity was assessed in NI and irradiated OE podocytes with or without C1P pre-treatment via MTT assay (Fig. 14). At 24hrs post-IR, cytotoxicity in the radioresistant, non-treated OE podocytes was ($8\pm 1\%$) relatively to the non-irradiated, non-treated group (NI, NT). Pre-treatment with C1P in NI OE cells resulted in cytotoxicity of ($22\pm 2\%$). Together, pre-treatment with C1P and irradiation raised cytotoxicity to ($38\pm 2\%$, $p < 0.0001$). These results suggest that C1P could be a potential key player in podocytes injury upon irradiation.

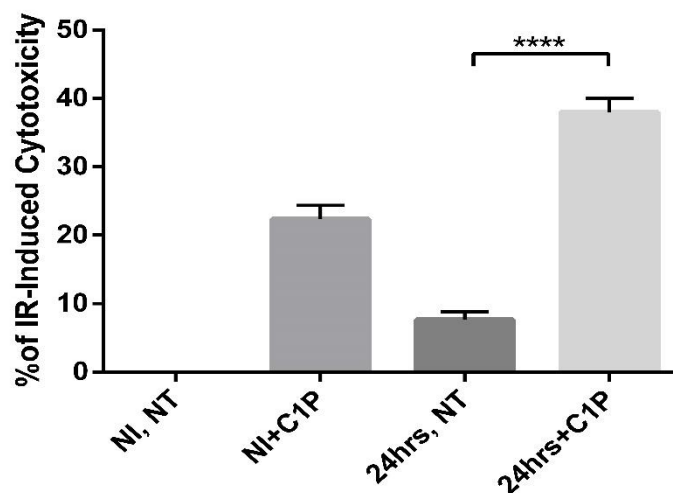


Figure 14: Exogenous C1P radiosensitizes SMPDL3b overexpressors. MTT survival assay was applied for C1P treated and non-treated (NT) OE podocytes with or without exposure to 2Gy X-rays. MTT assay was carried after 24hrs in irradiated groups. Results were obtained by spectrophotometry and expressed as percentages of IR-induced cytotoxicity relative to the non-irradiated, non-treated (NI, NT) group. Results represent the mean \pm SEM of 3 independent experiments.

H. ZOPRA pre-treatment radioprotects WT podocytes

Previous studies have shown that ZOPRA pre-treatment which is a combination of zoledronate (a bisphosphonate) and pravastatin (a cholesterol lowering statin) enhances ATM nuclear shuttling [46, 48, 154]. Therefore, we assessed the effect of ZOPRA treatment on WT and OE podocytes. In accordance with the previously published data, ZOPRA did not affect the kinetics of nuclear γ -H2AX and p-ATM foci in the radioresistant OE podocytes (data not shown). Moreover, single pre-treatment with either zoledronate or pravastatin did not produce any significant effect in both cell lines (data not shown).

1. Kinetics of γ -H2AX Foci Appearance/ Disappearance in ZOPRA treated and non-treated WT podocytes

We assessed the kinetics of DSBs recognition and repair by quantifying γ -H2AX foci in NI and irradiated WT cells, with or without ZOPRA pre-treatment, at 10min, 1hr, 4hrs and 24hrs post-IR (Fig. 15A). We found that a treated WT cell has, on average, a number of spontaneous nuclear γ -H2AX foci (1.7 ± 0.4) similar to a non-treated cell (2.3 ± 0.9). However, treated WT cells scored, on average, a significantly higher number of γ -H2AX foci/ cell (95 ± 9) than non-treated cells (77 ± 3 , $p<0.05$) at 10min post-IR (Fig. 15B). In addition, treated WT cells displayed on average a significantly lower number of residual γ -H2AX foci/ cell (7 ± 2) at 24hrs post-IR compared to non-treated cells (12 ± 0.3 , $p<0.01$) (Fig. 15C). Altogether, these results suggest that ZOPRA pre-treatment radioprotects WT podocytes by enhancing DSBs recognition and repair.

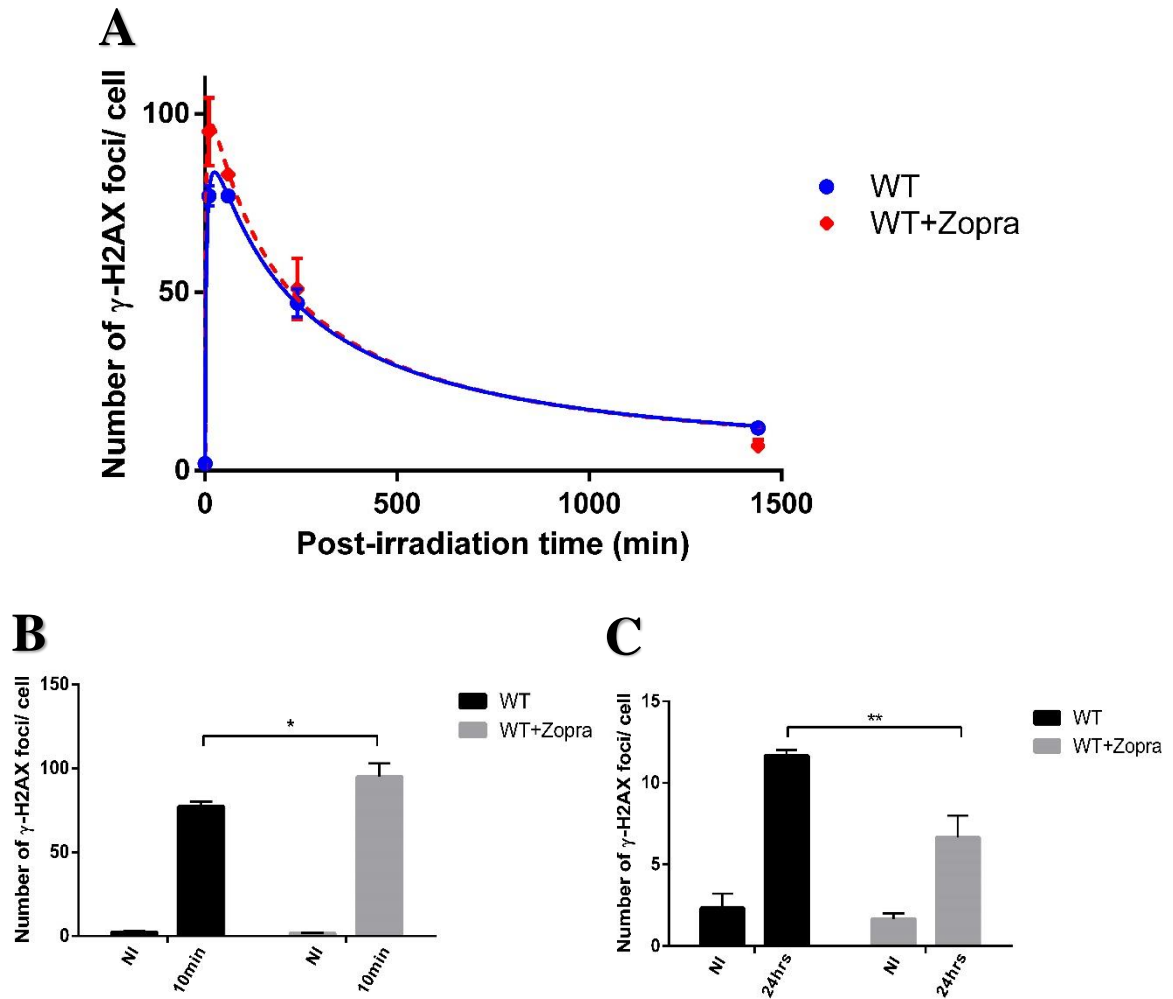


Figure 15: ZOPRA treatment enhances DSBs recognition and repair in WT podocytes. Immunofluorescence staining for γ -H2AX was applied for ZOPRA treated and non-treated WT podocytes which were exposed to 2Gy X-rays. (A) The numbers of γ -H2AX foci in both groups were plotted against post-irradiation times. Each plot represents the mean \pm SEM of 3 independent experiments. (B) and (C) The numbers of γ -H2AX foci assessed at 0, 10min and 24hrs post-IR in panels (A) are reported in histograms.

2. Kinetics of p-ATM Foci Appearance/ Disappearance in ZOPRA treated and non-treated WT podocytes

In order to check the effect of ZOPRA on ATM nuclear shuttling, we assessed the kinetics of p-ATM foci in NI and irradiated WT cells, with or without ZOPRA pre-treatment, at 10min, 1hr, 4hrs, and 24hrs post-IR (Fig. 16A). We found that a treated

WT cell has on average a number of spontaneous nuclear p-ATM foci (1.3 ± 0.8) similar to a non-treated cell (1.7 ± 0.3). However, treated WT cells scored, on average, a significantly higher number of p-ATM foci/ cell (90 ± 3) than non-treated cells (77 ± 2 , $p < 0.001$) at 10min post-irradiation (Fig. 16B). Both groups scored their maximal number of p-ATM foci at 10min post-irradiation. These results suggest that ZOPRA pre-treatment accelerates ATM nuclear shuttling in WT podocytes.

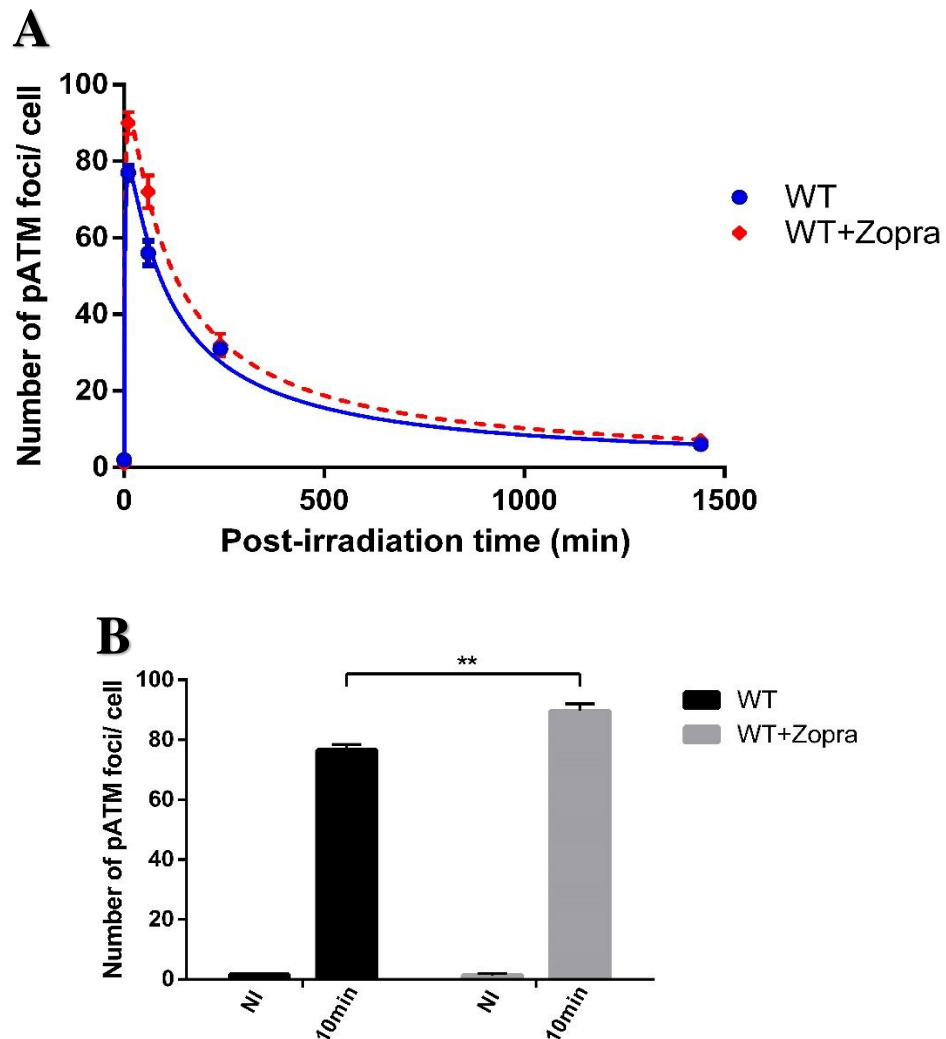


Figure 16: ZOPRA treatment accelerates ATM nuclear shuttling in WT podocytes. Immunofluorescence staining for p-ATM was applied for ZOPRA treated and non-treated WT podocytes which were exposed to 2Gy X-rays. (A) The numbers of p-ATM foci in both groups were plotted against post-irradiation times. Each plot represents the mean \pm SEM of 3 independent experiments. (B) The numbers of p-ATM foci assessed at 0 and 10min post-irradiation in panels (A) are reported in histograms.

3. Effect of ZOPRA treatment on WT podocytes viability

We were next interested in assessing the effect of ZOPRA pre-treatment on WT podocytes viability post-irradiation. For this purpose, cytotoxicity was assessed in NI and irradiated WT podocytes with or without ZOPRA pre-treatment via MTT assay (Fig. 17). At 24hrs post-irradiation, cytotoxicity in non-treated WT podocytes reached (21±4%) relatively to the non-irradiated, non-treated group (NI, NT). However, Pretreatment with ZOPRA reduced IR-induced cytotoxicity to (4±2%, $p<0.001$). These results suggest that ZOPRA radioprotects WT podocytes through enhanced DSBs recognition and repair.

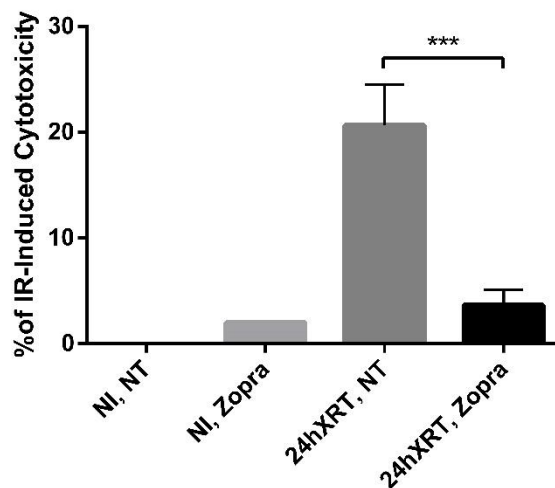


Figure 17: ZOPRA treatment radioprotects WT podocytes. MTT survival assay was applied for ZOPRA treated and non-treated (NT) WT podocytes with or without exposure to 2Gy X-rays. MTT assay was carried after 24hrs in irradiated groups. Results were obtained by spectrophotometry and expressed as percentages of IR-induced cytotoxicity relative to the non-irradiated, non-treated (NI, NT) group. Results represent the mean \pm SEM of 3 independent experiments.

CHAPTER IV

DISCUSSION

Radiation-induced nephropathy remains a challenging complication for cancer patients who receive abdominal and paraspinal radiotherapy (RT). Tumorcidal radiation doses often exceed the kidneys' tolerance threshold leaving patients at risk for developing renal dysfunction [155, 156]. Therefore, unraveling the molecular mechanisms involved in the development of radiation-induced kidneys' collateral damage is clinically valuable. It paves the path for developing pharmacological interventions that can protect patients from the lethal effects of radiation-induced nephrotoxicity.

It has been previously demonstrated that the glomerulus is the major culprit in radiation nephropathy [135]. In effect, podocytes are key players involved in the development of proteinuria in glomerular diseases [132] owing to the disruption of their actin cytoskeleton integrity [136]. Multiple studies have emphasized the role of sphingolipids in maintaining normal podocytes function [137-139]. The specific expression of the lipid modifying enzyme, SMPDL3b, in podocytes was reported to be a modulator of the activity of acid sphingomyelinase and stress signaling [143]. Strong evidence suggests that the modulation of SMPDL3b, albeit in different manners, is involved in multiple glomerular diseases by compromising the normal functioning of podocytes [143]. Our group has previously demonstrated that IR-induced loss of SMPDL3b leads to podocytes dysfunction by disrupting their sphingolipid homeostasis [132].

Our study identifies the sphingolipid-metabolizing enzyme, SMPDL3b, as a master regulator of the IR-induced DNA damage response in podocytes. It protects against IR-induced cell death by modulating ATM nuclear shuttling and maintaining nuclear sphingolipids homeostasis. Our findings suggest that SMPDL3b overexpression accelerates IR-induced ATM nuclear shuttling and subsequently DNA DSBs recognition and repair by potentially increasing the fluidity of the nuclear membrane and preserving the normal nuclear sphingolipid metabolism.

To our knowledge, we were the first to determine the number of IR-induced DSBs in human podocytes, which is around 55 DSBs/Gy. Previous studies conducted on human fibroblasts have reported approximately 40 DSBs/Gy [149, 157]. Unrepairable DSBs participate in IR-induced cell lethality. However, some unrepairable DSBs are tolerated by the cell and might not contribute to cell death depending on their localization inside the nucleus, chromatin condensation events and radiosensitivity [32].

IR induces the monomerization of cytoplasmic ATM dimers by oxidation. Subsequently, ATM dimers will shuttle into the nucleus to phosphorylate the histone variant H2AX at the site of damage. This step will ensure NHEJ-mediated DSBs recognition. Therefore, DSBs recognition may be influenced by the diffusion of p-ATM monomers as well as ATM re-dimerization or re-association with certain cytoplasmic proteins [32, 44, 46].

We next showed that wild-type human podocytes display significant radiosensitivity associated with unrepaired DSBs, delayed ATM nuclear shuttling, and increased IR-induced cell lethality (Fig. 5, 7, 8 and 9). This increased radiosensitivity was reversed by SMPDL3b overexpression which was previously demonstrated to

confer radioresistance in podocytes [132]. It reduced significantly the amount of unrepaired DSBs, accelerated ATM nuclear shuttling, and protected against IR-induced cell lethality (Fig. 5, 7, 8 and 9). These results unravel a novel role of SMPDL3b in modulating the DNA damage response. However, we noticed that p-ATM monomers are more abundant in the nuclear fractions of non-irradiated OE than in WT podocytes (Fig. 8). This can be potentially explained by the increased nuclear membrane fluidity in OE (discussed later). Thus, in order to determine whether the spontaneous nuclear levels of ATM monomers predict radiosensitivity and hence affect DSBs recognition and repair post-IR, we still need to validate our results by applying an ELISA-based assay. It will enable us to quantify accurately the amounts of active nuclear ATM monomers in both cell lines before and after irradiation.

Our results also show that IR induces a fast translocation of SMPDL3b from the lipid rafts of the podocytes' plasma membrane to the nuclear and perinuclear region. The protein also gets noticeably down-regulated there starting at 4hrs post-IR (Fig. 10) in agreement with the western blot results previously reported [132]. This ultimately leads to the disruption of the balanced sphingolipid metabolic pathway altering the levels of nuclear sphingolipid metabolites. The mechanisms by which SMPDL3b is translocated and degraded remain to be fully elucidated.

We next assessed the differences between OE and WT podocytes regarding the levels of nuclear sphingolipids before and after irradiation. We found that SMPDL3b overexpression resulted in decreased basal levels of total nuclear C1P and ceramides which remained stable post-irradiation (Fig. 11A-B). These results were in accordance with the newly published data which proved that SMPDL3b overexpression down-regulates C1P without changing the ceramide content, probably due to its fast

metabolism [144]. C1P was suggested to regulate cell proliferation and inhibit apoptosis [158-161], control phagocytosis [162, 163], and regulate inflammatory responses [164, 165]. However, it is still debatable whether it acts as a pro-inflammatory or anti-inflammatory signaling molecule. In order to mimic the up-regulation of C1P in WT podocytes, we administered C1P exogenously to OE. Interestingly, C1P pre-treatment sensitizes OE cells to RT by impairing DSBs recognition and repair, delaying ATM nuclear shuttling, and increasing IR-induced cytotoxicity (Fig. 12, 13, and 14). Thus, in our model, C1P is favoring IR-induced cell death. Further investigations should be done to determine if SMPDL3b converts synthetic C1P into ceramides that might be responsible for the negative impact. Our group previously demonstrated that SMPDL3b overexpression resulted in increased basal levels of the pro-survival S1P which were maintained post-irradiation [132]. However, in our study, we could not detect nuclear S1P in any of the cell lines. Given that, it is plausible that SMPDL3b regulates the levels of the bioactive sphingolipid metabolites: ceramides, C1P and S1P, which can be interconverted rapidly and determine the fate of the cell.

Sphingomyelin (SM) is the most abundant nuclear sphingolipid. It is primarily found in the nuclear envelope and to a lesser extent in nuclear matrix and chromatin [166]. Sphingomyelinases, which were also detected in the nuclear envelope [167], nuclear matrix [168], and chromatin [169] of rat liver nuclei, metabolize SM into ceramides. In turn, ceramides can be converted into SM by the action of SM synthase, detected in the nuclear envelope and chromatin [170]. Besides SM, the nuclear membrane contains abundantly phosphatidylcholine (PC) and cholesterol (CHO). These are the most important lipids that regulate the structure, function, and fluidity of the nuclear membrane [171]. SM and CHO increase a membrane's rigidity, whereas PC

increases its fluidity [172]. Therefore, a high SM-CHO/ PC ratio will decrease the fluidity of the nuclear membrane and vice versa. As the fluidity of the nuclear membrane increases, the size of the nuclear pores changes allowing increased nuclear-cytoplasmic transport such as that of mRNA during cell proliferation [171]. After analyzing the content of nuclear sphingomyelin in both cell lines (Fig. 11C), we found that nuclear SM does not change significantly post-irradiation. However, SMPDL3b overexpressors displayed significantly decreased basal levels of nuclear SM compared to WT podocytes. This low content of nuclear SM in OE can be potentially explained by an increased sphingomyelinase activity mediated by SMPDL3b. These results can potentially explain the reason behind the increased nuclear membrane fluidity in SMPDL3b overexpressors which has played a key role in accelerating ATM nuclear shuttling and subsequently enhancing DSBs repair. However, further assessments of the nuclear membrane lipid contents and fluidity of both cell lines should be performed.

Previous studies have shown that ZOPRA treatment, which is a combination of zoledronate (a bisphosphonate) and pravastatin (a cholesterol lowering statin), enhances ATM nuclear shuttling [46, 48, 154]. In our study, pre-treatment with ZOPRA gave promising results in WT podocytes. Similarly to SMPDL3b overexpression, it conferred radioresistance by accelerating ATM nuclear shuttling, enhancing DSBs recognition and repair, and protecting against IR-induced cytotoxicity (Fig. 15, 16, and 17). Multiple studies have been conducted to unravel the mechanism of action of ZOPRA on ATM nuclear shuttling in fibroblasts. It was suggested that ZOPRA inhibits nuclear membrane farnesylation and geranylgeranylation of prelamin A and its truncated form (progerin) [154]. Then, it was suggested to mitigate some of the clinical complications of Huntington disease such as osteoporosis and cholesterol dysregulation besides

accelerating ATM shuttling in fibroblasts having mutated huntingtin protein [46]. Later, it was shown to accelerate ATM shuttling in fibroblasts derived from patients with tuberous sclerosis in which TSC complexes sequester cytoplasmic ATM monomers and impede their shuttling [48]. Pravastatin inhibits HMG-CoA reductase at the top of the mevalonate pathway whereas zoledronate inhibits isopentenyl pyrophosphate isomerase and farnesyl pyrophosphate synthase at the bottom of the pathway [173]. The combination of these two drugs block the farnesylation and geranylgeranylation of membrane proteins, thus impeding alternative prenylation events [154]. However, besides the effect of this combined drug on membrane farnesylation, ZOPRA might induce further effects through the usual functions of statins and bisphosphonates. Statins are cholesterol lowering drugs that were proven to inhibit cholesterol synthesis, modulate immunological responses, and attack the proteasomal machinery [174, 175]. Bisphosphonates are anti-osteoporotic drugs that regulate calcium homeostasis and block angiogenesis independently of the mevalonate pathway [176, 177]. In fact, both drugs act synergistically in order to induce a significant acceleration of ATM nuclear shuttling. This combination might potentially affect nuclear membrane fluidity by lowering its cholesterol content, and therefore disrupting the SM-CHO/ PC ratio besides inhibiting membrane farnesylation. However, the exact mechanisms of action of ZOPRA in podocytes remain to be established.

Nevertheless, our study does not stand without its limitations. We focused only on one component of the glomerular filtration barrier, the podocytes. In order to validate our *in vitro* data and elucidate the cell-to-cell interactions that take place in IR-targeted renal glomeruli, further investigations are needed. These should focus on glomerular endothelial cells and *in vivo* animal models. Besides, our study only tackled the γ -H2AX

mediated NHEJ repair of DSBs without taking into consideration other H2AX independent mechanisms of DSBs repair, such as the MRE11 pathway.

Our future work will focus on exploring the holistic role of the SMPDL3b-mediated DNA repair pathway in an effort to reveal its position in the network of events that occur after collateral kidney irradiation, and trying to unravel the best pharmacological interventions that can yield promising outcomes.

In a nutshell, the current study identifies a novel role for SMPDL3b in mediating IR-induced DNA damage response through a chain of cellular events. SMPDL3b modulates ATM nuclear shuttling through the potential regulation of nuclear membrane fluidity and nuclear sphingolipids metabolism. It subsequently affects DSBs repair and podocytes' survival. Therefore, our study paves the path for identifying novel therapeutic targets which might help delivering tumoricidal doses while preventing radiation nephropathy. A hypothetical model illustrates our findings in **Fig.18**.

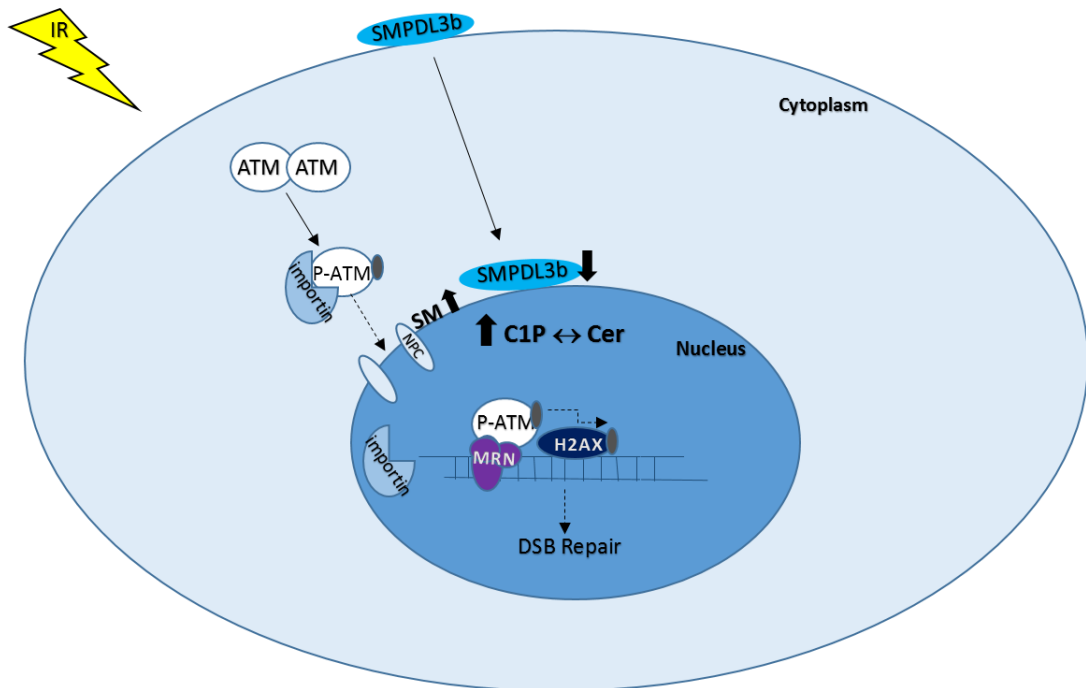


Figure 18: Model of IR-induced DNA damage response in podocytes. The modulation of SMPDL3b plays a key role in disrupting the DDR post-IR. This triggers changes in nuclear membrane fluidity and nuclear sphingolipids, including SM, C1P, and Ceramide (Cer) resulting in delayed ATM nuclear shuttling and subsequently delayed DSBs recognition and repair. Dashed arrows represent delayed actions.

REFERENCES

1. *Cancer facts & figures 2019*. American Cancer Society 2019.
2. Bray, F., et al., *Global cancer statistics 2018: GLOBOCAN estimates of incidence and mortality worldwide for 36 cancers in 185 countries*. CA: a cancer journal for clinicians, 2018. **68**(6): p. 394-424.
3. Torre, L.A., et al., *Global cancer incidence and mortality rates and trends—an update*. Cancer Epidemiology and Prevention Biomarkers, 2016. **25**(1): p. 16-27.
4. You, W. and M. Henneberg, *Cancer incidence increasing globally: the role of relaxed natural selection*. Evolutionary applications, 2018. **11**(2): p. 140-152.
5. Baskar, R., et al., *Cancer and radiation therapy: current advances and future directions*. International journal of medical sciences, 2012. **9**(3): p. 193.
6. Barnett, G.C., et al., *Normal tissue reactions to radiotherapy: towards tailoring treatment dose by genotype*. Nature Reviews Cancer, 2009. **9**(2): p. 134.
7. Deloch, L., et al., *Modern radiotherapy concepts and the impact of radiation on immune activation*. Frontiers in oncology, 2016. **6**: p. 141.
8. Eriksson, D. and T. Stigbrand, *Radiation-induced cell death mechanisms*. Tumor Biology, 2010. **31**(4): p. 363-372.
9. Balcer-Kubiczek, E., *Apoptosis in radiation therapy: a double-edged sword*. Experimental oncology, 2012.
10. Baskar, R., *Emerging role of radiation induced bystander effects: Cell communications and carcinogenesis*. Genome integrity, 2010. **1**(1): p. 13.
11. Hall, E.J., *Cancer caused by x-rays—a random event?* The Lancet Oncology, 2007. **8**(5): p. 369-370.
12. Schulz-Ertner, D. and H. Tsujii, *Particle radiation therapy using proton and heavier ion beams*. Journal of clinical oncology, 2007. **25**(8): p. 953-964.
13. Ma, C.M.C., R.L. Maughan, and C.G. Orton, *Within the next decade conventional cyclotrons for proton radiotherapy will become obsolete and replaced by far less expensive machines using compact laser systems for the acceleration of the protons*. Medical physics, 2006. **33**(3): p. 571-573.
14. Edeani, A., Cohen, E.P., *Chapter 10: Radiation Nephropathy*. American Society of Nephrology, 2016. **Onco-Nephrology Curriculum**
15. Orth, M., et al., *Current concepts in clinical radiation oncology*. Radiation and environmental biophysics, 2014. **53**(1): p. 1-29.
16. Muller-Runkel, R. and S. Vijayakumar, *Equivalent total doses for different fractionation schemes, based on the linear quadratic model*. Radiology, 1991. **179**(2): p. 573-577.
17. Dörr, W., M. Baumann, and T. Herrmann, *Nomenclature of modified fractionation protocols in radiotherapy*. Strahlentherapie und Onkologie: Organ der Deutschen Röntgengesellschaft...[et al], 1996. **172**(7): p. 353-355.
18. Jackson, S.P. and J. Bartek, *The DNA-damage response in human biology and disease*. Nature, 2009. **461**(7267): p. 1071.
19. Desouky, O., N. Ding, and G. Zhou, *Targeted and non-targeted effects of ionizing radiation*. Journal of Radiation Research and Applied Sciences, 2015. **8**(2): p. 247-254.
20. Saha, G.B., *Physics and radiobiology of nuclear medicine*. 2012: Springer Science & Business Media.

21. Hall, E.J. and A.J. Giaccia, *Radiobiology for the Radiologist*. Vol. 6. 2006: Lippincott Williams & Wilkins.
22. Azzam, E.I., J.-P. Jay-Gerin, and D. Pain, *Ionizing radiation-induced metabolic oxidative stress and prolonged cell injury*. *Cancer letters*, 2012. **327**(1-2): p. 48-60.
23. Negritto, C., *Repairing double-strand DNA breaks*. *Nat Educ*, 2010. **3**(9): p. 26.
24. Isaksson, M. and C.L. Raaf, *Environmental radioactivity and emergency preparedness*. 2017: CRC Press.
25. Thompson, L.H., *Recognition, signaling, and repair of DNA double-strand breaks produced by ionizing radiation in mammalian cells: the molecular choreography*. *Mutation Research/Reviews in Mutation Research*, 2012. **751**(2): p. 158-246.
26. Bauer, N.C., A.H. Corbett, and P.W. Doetsch, *The current state of eukaryotic DNA base damage and repair*. *Nucleic acids research*, 2015. **43**(21): p. 10083-10101.
27. Carroll, B., J.C. Donaldson, and L. Obeid, *Sphingolipids in the DNA damage response*. *Advances in biological regulation*, 2015. **58**: p. 38-52.
28. Jeggo, P. and M. Löbrich, *DNA double-strand breaks: their cellular and clinical impact?* *Oncogene*, 2007. **26**(56): p. 7717.
29. Woodbine, L., A.R. Gennery, and P.A. Jeggo, *The clinical impact of deficiency in DNA non-homologous end-joining*. *DNA repair*, 2014. **16**: p. 84-96.
30. Sonoda, E., et al., *Differential usage of non-homologous end-joining and homologous recombination in double strand break repair*. *DNA repair*, 2006. **5**(9-10): p. 1021-1029.
31. Beucher, A., et al., *ATM and Artemis promote homologous recombination of radiation-induced DNA double-strand breaks in G2*. *The EMBO journal*, 2009. **28**(21): p. 3413-3427.
32. Bodgi, L. and N. Foray, *The nucleo-shuttling of the ATM protein as a basis for a novel theory of radiation response: resolution of the linear-quadratic model*. *International journal of radiation biology*, 2016. **92**(3): p. 117-131.
33. Czornak, K., S. Chughtai, and K.H. Chrzanowska, *Mystery of DNA repair: the role of the MRN complex and ATM kinase in DNA damage repair*. *Journal of applied genetics*, 2008. **49**(4): p. 383-396.
34. Kastan, M.B., et al., *Participation of p53 protein in the cellular response to DNA damage*. *Cancer research*, 1991. **51**(23 Part 1): p. 6304-6311.
35. Goto, H., et al., *Novel regulation of checkpoint kinase 1: Is checkpoint kinase 1 a good candidate for anti-cancer therapy?* *Cancer science*, 2012. **103**(7): p. 1195-1200.
36. Dasika, G.K., et al., *DNA damage-induced cell cycle checkpoints and DNA strand break repair in development and tumorigenesis*. *oncogene*, 1999. **18**(55): p. 7883.
37. Paull, T.T., et al., *A critical role for histone H2AX in recruitment of repair factors to nuclear foci after DNA damage*. *Current Biology*, 2000. **10**(15): p. 886-895.
38. Rappold, I., et al., *Tumor suppressor p53 binding protein 1 (53BP1) is involved in DNA damage–signaling pathways*. *The Journal of cell biology*, 2001. **153**(3): p. 613-620.
39. Burma, S., et al., *ATM phosphorylates histone H2AX in response to DNA double-strand breaks*. *Journal of Biological Chemistry*, 2001. **276**(45): p. 42462-42467.
40. Ward, I.M. and J. Chen, *Histone H2AX is phosphorylated in an ATR-dependent manner in response to replicational stress*. *Journal of Biological Chemistry*, 2001. **276**(51): p. 47759-47762.
41. Ward, I.M., K. Minn, and J. Chen, *UV-induced ataxia-telangiectasia-mutated and Rad3-related (ATR) activation requires replication stress*. *Journal of Biological Chemistry*, 2004. **279**(11): p. 9677-9680.
42. Bakkenist, C.J. and M.B. Kastan, *DNA damage activates ATM through intermolecular autophosphorylation and dimer dissociation*. *Nature*, 2003. **421**(6922): p. 499.
43. Canman, C.E., et al., *Activation of the ATM kinase by ionizing radiation and phosphorylation of p53*. *Science*, 1998. **281**(5383): p. 1677-1679.

44. Bodgi, L., et al., *A single formula to describe radiation-induced protein relocalization: towards a mathematical definition of individual radiosensitivity*. Journal of theoretical biology, 2013. **333**: p. 135-145.
45. Ouenzar, F., M.J. Hendzel, and M. Weinfeld, *Shuttling towards a predictive assay for radiotherapy*. Translational Cancer Research, 2016. **5**(4): p. S742-S746.
46. Ferlazzo, M.L., et al., *Mutations of the Huntington's disease protein impact on the ATM-dependent signaling and repair pathways of the radiation-induced DNA double-strand breaks: Corrective effect of statins and bisphosphonates*. Molecular neurobiology, 2014. **49**(3): p. 1200-1211.
47. Pereira, S., et al., *Fast and binary assay for predicting radiosensitivity based on the theory of ATM nucleo-shuttling: Development, validation, and performance*. International Journal of Radiation Oncology* Biology* Physics, 2018. **100**(2): p. 353-360.
48. Ferlazzo, M.L., et al., *Radiobiological characterization of tuberous sclerosis: A delay in the nucleo-shuttling of ATM may be responsible for radiosensitivity*. Molecular neurobiology, 2018. **55**(6): p. 4973-4983.
49. Turesson, I., et al., *Prognostic factors for acute and late skin reactions in radiotherapy patients*. International Journal of Radiation Oncology* Biology* Physics, 1996. **36**(5): p. 1065-1075.
50. Gatti, R.A., *The inherited basis of human radiosensitivity*. Acta Oncologica, 2001. **40**(6): p. 702-711.
51. Granzotto, A., et al., *Influence of nucleoshuttling of the ATM protein in the healthy tissues response to radiation therapy: toward a molecular classification of human radiosensitivity*. International Journal of Radiation Oncology* Biology* Physics, 2016. **94**(3): p. 450-460.
52. Cornforth, M.N. and J.S. Bedford, *A quantitative comparison of potentially lethal damage repair and the rejoining of interphase chromosome breaks in low passage normal human fibroblasts*. Radiation research, 1987. **111**(3): p. 385-405.
53. Jeggo, P., *Identification of genes involved in repair of DNA double-strand breaks in mammalian cells*. Radiation research, 1998. **150**(5s): p. S80-S91.
54. Deschavanne, P.J. and B. Fertil, *A review of human cell radiosensitivity in vitro*. International Journal of Radiation Oncology* Biology* Physics, 1996. **34**(1): p. 251-266.
55. Foray, N., et al., *A subset of ATM-and ATR-dependent phosphorylation events requires the BRCA1 protein*. The EMBO journal, 2003. **22**(11): p. 2860-2871.
56. Löbrich, M. and P.A. Jeggo, *The two edges of the ATM sword: co-operation between repair and checkpoint functions*. Radiotherapy and oncology, 2005. **76**(2): p. 112-118.
57. Morgan, J.L., T.M. Holcomb, and R.W. Morrissey, *Radiation reaction in ataxia telangiectasia*. American journal of diseases of children, 1968. **116**(5): p. 557-558.
58. Pietrucha, B.M., et al., *Ataxia-telangiectasia with hyper-IgM and Wilms tumor: fatal reaction to irradiation*. Journal of pediatric hematology/oncology, 2010. **32**(1): p. e28-e30.
59. Chistiakov, D.A., N.V. Voronova, and A.P. Chistiakov, *Ligase IV syndrome*. European journal of medical genetics, 2009. **52**(6): p. 373-378.
60. Hollstein, M., et al., *p53 mutations in human cancers*. Science, 1991. **253**(5015): p. 49-53.
61. Soussi, T. and C. Bérout, *Assessing TP53 status in human tumours to evaluate clinical outcome*. Nature Reviews Cancer, 2001. **1**(3): p. 233.
62. Soussi, T. and G. Lozano, *p53 mutation heterogeneity in cancer*. Biochemical and biophysical research communications, 2005. **331**(3): p. 834-842.
63. Helton, E.S. and X. Chen, *p53 modulation of the DNA damage response*. Journal of cellular biochemistry, 2007. **100**(4): p. 883-896.

64. Igney, F.H. and P.H. Krammer, *Death and anti-death: tumour resistance to apoptosis*. Nature Reviews Cancer, 2002. **2**(4): p. 277.
65. Lauber, K., et al., *Dying cell clearance and its impact on the outcome of tumor radiotherapy*. Frontiers in oncology, 2012. **2**: p. 116.
66. Schmitt, C.A., *Senescence, apoptosis and therapy—cutting the lifelines of cancer*. Nature Reviews Cancer, 2003. **3**(4): p. 286.
67. Dewey, W., *Radiation-induced apoptosis: Relevance to radiotherapy*. Int J Radiat Oncol Biol Phys, 1991. **21**: p. 109-122.
68. Galluzzi, L., et al., *Cell death modalities: classification and pathophysiological implications*. 2007, Nature Publishing Group.
69. Eriksson, D., et al., *Combined low dose radio-and radioimmunotherapy of experimental HeLa Hep 2 tumours*. European journal of nuclear medicine and molecular imaging, 2003. **30**(6): p. 895-906.
70. Eriksson, D., et al., *Cell cycle disturbances and mitotic catastrophes in HeLa Hep2 cells following 2.5 to 10 Gy of ionizing radiation*. Clinical Cancer Research, 2007. **13**(18): p. 5501s-5508s.
71. Castedo, M. and G. Kroemer, *Mitotic catastrophe: a special case of apoptosis*. Journal de la Societe de biologie, 2004. **198**(2): p. 97-103.
72. Erenpreisa, J., et al., *Segregation of genomes in polyploid tumour cells following mitotic catastrophe*. Cell biology international, 2005. **29**(12): p. 1005-1011.
73. Roninson, I.B., E.V. Broude, and B.-D. Chang, *If not apoptosis, then what? Treatment-induced senescence and mitotic catastrophe in tumor cells*. Drug Resistance Updates, 2001. **4**(5): p. 303-313.
74. Ianzini, F., et al., *Lack of p53 function promotes radiation-induced mitotic catastrophe in mouse embryonic fibroblast cells*. Cancer cell international, 2006. **6**(1): p. 11.
75. Bourke, E., et al., *DNA damage induces Chk1-dependent centrosome amplification*. EMBO reports, 2007. **8**(6): p. 603-609.
76. Dodson, H., S.P. Wheatley, and C.G. Morrison, *Involvement of centrosome amplification in radiation-induced mitotic catastrophe*. Cell Cycle, 2007. **6**(3): p. 364-370.
77. Kawamura, K., et al., *Centrosome hyperamplification and chromosomal damage after exposure to radiation*. Oncology, 2004. **67**(5-6): p. 460-470.
78. Kawamura, K., et al., *Induction of centrosome amplification in p53 siRNA-treated human fibroblast cells by radiation exposure*. Cancer science, 2006. **97**(4): p. 252-258.
79. Hanashiro, K., et al., *Roles of cyclins A and E in induction of centrosome amplification in p53-compromised cells*. Oncogene, 2008. **27**(40): p. 5288.
80. Vakifahmetoglu, H., M. Olsson, and B. Zhivotovsky, *Death through a tragedy: mitotic catastrophe*. Cell death and differentiation, 2008. **15**(7): p. 1153.
81. Kroemer, G., et al., *Classification of cell death: recommendations of the Nomenclature Committee on Cell Death 2009*. Cell death and differentiation, 2009. **16**(1): p. 3.
82. Brandsma, D., et al., *Clinical features, mechanisms, and management of pseudoprogression in malignant gliomas*. The lancet oncology, 2008. **9**(5): p. 453-461.
83. Krysko, O., et al., *Many faces of DAMPs in cancer therapy*. Cell death & disease, 2013. **4**(5): p. e631.
84. Proskuryakov, S.Y., A.G. Konoplyannikov, and V.L. Gabai, *Necrosis: a specific form of programmed cell death? Experimental cell research*, 2003. **283**(1): p. 1-16.
85. Cohen-Jonathan, E., E.J. Bernhard, and W.G. McKenna, *How does radiation kill cells? Current opinion in chemical biology*, 1999. **3**(1): p. 77-83.
86. Batalni, J.P., et al., *Desmoid tumors in adults: the role of radiotherapy in their management*. The American journal of surgery, 1988. **155**(6): p. 754-760.

87. Cox, J.D. and R.W. Kline, *Do prostatic biopsies 12 months or more after external irradiation for adenocarcinoma, Stage III, predict long-term survival?* International Journal of Radiation Oncology* Biology* Physics, 1983. **9**(3): p. 299-303.
88. Shay, J.W. and I.B. Roninson, *Hallmarks of senescence in carcinogenesis and cancer therapy.* Oncogene, 2004. **23**(16): p. 2919.
89. Gewirtz, D.A., S.E. Holt, and L.W. Elmore, *Accelerated senescence: an emerging role in tumor cell response to chemotherapy and radiation.* Biochemical pharmacology, 2008. **76**(8): p. 947-957.
90. Rodier, F., et al., *Persistent DNA damage signalling triggers senescence-associated inflammatory cytokine secretion.* Nature cell biology, 2009. **11**(8): p. 973.
91. Suzuki, K., et al., *Radiation-induced senescence-like growth arrest requires TP53 function but not telomere shortening.* Radiation research, 2001. **155**(1): p. 248-253.
92. Abou Daher, A., et al., *Translational aspects of sphingolipid metabolism in renal disorders.* International journal of molecular sciences, 2017. **18**(12): p. 2528.
93. Hannun, Y.A. and L.M. Obeid, *Principles of bioactive lipid signalling: lessons from sphingolipids.* Nature reviews Molecular cell biology, 2008. **9**(2): p. 139.
94. Gault, C.R., L.M. Obeid, and Y.A. Hannun, *An overview of sphingolipid metabolism: from synthesis to breakdown,* in *Sphingolipids as Signaling and Regulatory Molecules.* 2010, Springer. p. 1-23.
95. Boath, A., et al., *Regulation and traffic of ceramide 1-phosphate produced by ceramide kinase comparative analysis to glucosylceramide and sphingomyelin.* Journal of Biological Chemistry, 2008. **283**(13): p. 8517-8526.
96. Ogawa, C., et al., *Identification and characterization of a novel human sphingosine-1-phosphate phosphohydrolase, hSPP2.* Journal of Biological Chemistry, 2003. **278**(2): p. 1268-1272.
97. Mandala, S.M., et al., *Molecular cloning and characterization of a lipid phosphohydrolase that degrades sphingosine-1-phosphate and induces cell death.* Proceedings of the National Academy of Sciences, 2000. **97**(14): p. 7859-7864.
98. Pyne, S., et al., *Lipid phosphate phosphatases and lipid phosphate signalling.* 2005, Portland Press Limited.
99. Ikeda, M., A. Kihara, and Y. Igarashi, *Sphingosine-1-phosphate lyase SPL is an endoplasmic reticulum-resident, integral membrane protein with the pyridoxal 5'-phosphate binding domain exposed to the cytosol.* Biochemical and biophysical research communications, 2004. **325**(1): p. 338-343.
100. Obanda, D.N., et al., *Modulation of sphingolipid metabolism with calorie restriction enhances insulin action in skeletal muscle.* The Journal of nutritional biochemistry, 2015. **26**(7): p. 687-695.
101. Reynolds, C.P., B.J. Maurer, and R.N. Kolesnick, *Ceramide synthesis and metabolism as a target for cancer therapy.* Cancer letters, 2004. **206**(2): p. 169-180.
102. Gault, C.R. and L.M. Obeid, *Still benched on its way to the bedside: sphingosine kinase 1 as an emerging target in cancer chemotherapy.* Critical reviews in biochemistry and molecular biology, 2011. **46**(4): p. 342-351.
103. Dbaiibo, G.S., et al., *p53-dependent ceramide response to genotoxic stress.* The Journal of clinical investigation, 1998. **102**(2): p. 329-339.
104. Vit, J.-P. and F. Rosselli, *Role of the ceramide-signaling pathways in ionizing radiation-induced apoptosis.* Oncogene, 2003. **22**(54): p. 8645.
105. Sawada, M., et al., *p53 regulates ceramide formation by neutral sphingomyelinase through reactive oxygen species in human glioma cells.* Oncogene, 2001. **20**(11): p. 1368.

106. Corcoran, C.A., et al., *Neutral sphingomyelinase-3 is a DNA damage and nongenotoxic stress-regulated gene that is deregulated in human malignancies*. *Molecular Cancer Research*, 2008. **6**(5): p. 795-807.
107. Ravid, T., et al., *Ceramide accumulation precedes caspase-3 activation during apoptosis of A549 human lung adenocarcinoma cells*. *American Journal of Physiology-Lung Cellular and Molecular Physiology*, 2003. **284**(6): p. L1082-L1092.
108. Dbaibo, G.S., et al., *Retinoblastoma gene product as a downstream target for a ceramide-dependent pathway of growth arrest*. *Proceedings of the National Academy of Sciences*, 1995. **92**(5): p. 1347-1351.
109. Phillips, D., et al., *Ceramide-induced G 2 arrest in rhabdomyosarcoma (RMS) cells requires p21 Cip1/Waf1 induction and is prevented by MDM2 overexpression*. *Cell death and differentiation*, 2007. **14**(10): p. 1780.
110. Kastan, M.B., et al., *A mammalian cell cycle checkpoint pathway utilizing p53 and GADD45 is defective in ataxia-telangiectasia*. *Cell*, 1992. **71**(4): p. 587-597.
111. Taha, T.A., et al., *Down-regulation of Sphingosine Kinase-1 by DNA Damage DEPENDENCE ON PROTEASES AND p53*. *Journal of Biological Chemistry*, 2004. **279**(19): p. 20546-20554.
112. Maceyka, M., et al., *SphK1 and SphK2, sphingosine kinase isoenzymes with opposing functions in sphingolipid metabolism*. *Journal of Biological Chemistry*, 2005. **280**(44): p. 37118-37129.
113. Sankala, H.M., et al., *Involvement of sphingosine kinase 2 in p53-independent induction of p21 by the chemotherapeutic drug doxorubicin*. *Cancer research*, 2007. **67**(21): p. 10466-10474.
114. Johnson, K.R., et al., *Role of human sphingosine-1-phosphate phosphatase 1 in the regulation of intra-and extracellular sphingosine-1-phosphate levels and cell viability*. *Journal of Biological Chemistry*, 2003. **278**(36): p. 34541-34547.
115. Oskouian, B., et al., *Sphingosine-1-phosphate lyase potentiates apoptosis via p53-and p38-dependent pathways and is down-regulated in colon cancer*. *Proceedings of the National Academy of Sciences*, 2006. **103**(46): p. 17384-17389.
116. Edsall, D.L., *The attitude of the clinician in regard to exposing patients to the x-ray*. *Journal of the American Medical Association*, 1906. **47**(18): p. 1425-1429.
117. Domagk, G., *Röntgenstrahlenschädigungen der Niere beim Menschen*. *Med. Klin*, 1927. **23**: p. 345.
118. Dawson, L.A., et al., *Radiation-associated kidney injury*. *International Journal of Radiation Oncology* Biology* Physics*, 2010. **76**(3): p. S108-S115.
119. Cassady, J.R., *Clinical radiation nephropathy*. *International Journal of Radiation Oncology* Biology* Physics*, 1995. **31**(5): p. 1249-1256.
120. Cohen, E.P., P. Pais, and J.E. Moulder. *Chronic kidney disease after hematopoietic stem cell transplantation*. in *Seminars in nephrology*. 2010. Elsevier.
121. Luxton, R., *Radiation nephritis: a long-term study of 54 patients*. *Lancet (England)*, 1961. **2**.
122. LUXTON, R.W., *RADIATION NEPHRITIS1*. *QJM: An International Journal of Medicine*, 1953. **22**(2): p. 215-242.
123. Dawson, L.A., A. Horgan, and E.P. Cohen, *Kidney and ureter*, in *ALERT• Adverse Late Effects of Cancer Treatment*. 2014, Springer. p. 443-464.
124. Cohen, E.P., *Radiation nephropathy after bone marrow transplantation*. *Kidney international*, 2000. **58**(2): p. 903-918.
125. Baldwin, J.N. and J.W. Hagstrom, *Acute radiation nephritis*. *California medicine*, 1962. **97**(6): p. 359.

126. Cruz, D.N., M.A. Perazella, and R.L. Mahnensmith, *Bone marrow transplant nephropathy: a case report and review of the literature*. Journal of the American Society of Nephrology, 1997. **8**(1): p. 166-173.
127. Rubin, P. and G.W. Casarett, *CLINICAL RADIATION PATHOLOGY. VOLUME II*. 1968.
128. Verheij, M., et al., *Evidence for a renovascular component in hypertensive patients with late radiation nephropathy*. International Journal of Radiation Oncology* Biology* Physics, 1994. **30**(3): p. 677-683.
129. Krochak, R.J. and D.G. Baker, *Radiation Nephritis Clinical manifestations and pathophysiologic mechanisms*. Urology, 1986. **27**(5): p. 389-393.
130. Cohen, E.P., et al., *Clinical course of late-onset bone marrow transplant nephropathy*. Nephron, 1993. **64**(4): p. 626-635.
131. Cohen, E.P. and M.E. Robbins. *Radiation nephropathy*. in *Seminars in nephrology*. 2003. Elsevier.
132. Ahmad, A., et al., *Sphingomyelinase-like phosphodiesterase 3b mediates radiation-induced damage of renal podocytes*. The FASEB Journal, 2016. **31**(2): p. 771-780.
133. White, D.C., *The histopathologic basis for functional decrements in late radiation injury in diverse organs*. Cancer, 1976. **37**(S2): p. 1126-1143.
134. Scharpfenecker, M., et al., *The TGF- β co-receptor endoglin regulates macrophage infiltration and cytokine production in the irradiated mouse kidney*. Radiotherapy and Oncology, 2012. **105**(3): p. 313-320.
135. Stephens, L.C., et al., *Radiation nephropathy in the rhesus monkey: morphometric analysis of glomerular and tubular alterations*. International Journal of Radiation Oncology* Biology* Physics, 1995. **31**(4): p. 865-873.
136. Ruotsalainen, V., et al., *Nephrin is specifically located at the slit diaphragm of glomerular podocytes*. Proceedings of the National Academy of Sciences, 1999. **96**(14): p. 7962-7967.
137. Lennon, R., et al., *Saturated fatty acids induce insulin resistance in human podocytes: implications for diabetic nephropathy*. Nephrology Dialysis Transplantation, 2009. **24**(11): p. 3288-3296.
138. Basic-Jukic, N., et al., *Renal complications of Fabry disease*. Current pharmaceutical design, 2013. **19**(33): p. 6046-6050.
139. Merscher, S. and A. Fornoni, *Podocyte pathology and nephropathy—sphingolipids in glomerular diseases*. Frontiers in endocrinology, 2014. **5**: p. 127.
140. Pavenstadt, H., W. Kriz, and M. Kretzler, *Cell biology of the glomerular podocyte*. Physiological reviews, 2003. **83**(1): p. 253-307.
141. Cellesi, F., M. Li, and M.P. Rastaldi, *Podocyte injury and repair mechanisms*. Current opinion in nephrology and hypertension, 2015. **24**(3): p. 239-244.
142. Nagata, M., *Podocyte injury and its consequences*. Kidney international, 2016. **89**(6): p. 1221-1230.
143. Fornoni, A., et al., *Rituximab targets podocytes in recurrent focal segmental glomerulosclerosis*. Science translational medicine, 2011. **3**(85): p. 85ra46-85ra46.
144. Mitrofanova, A., et al., *SMPDL3b modulates insulin receptor signaling in diabetic kidney disease*. Nature Communications, 2019. **10**(1): p. 2692.
145. Perosa, F., et al., *Generation of biologically active linear and cyclic peptides has revealed a unique fine specificity of rituximab and its possible cross-reactivity with acid sphingomyelinase-like phosphodiesterase 3b precursor*. Blood, 2006. **107**(3): p. 1070-1077.
146. Tasaki, M., et al., *Rituximab treatment prevents the early development of proteinuria following pig-to-baboon xeno-kidney transplantation*. Journal of the American Society of Nephrology, 2014. **25**(4): p. 737-744.

147. Bielawski, J., et al., *Simultaneous quantitative analysis of bioactive sphingolipids by high-performance liquid chromatography-tandem mass spectrometry*. *Methods*, 2006. **39**(2): p. 82-91.
148. Rothkamm, K. and M. Löbrich, *Evidence for a lack of DNA double-strand break repair in human cells exposed to very low x-ray doses*. *Proceedings of the National Academy of Sciences*, 2003. **100**(9): p. 5057-5062.
149. FORAY, A.P., G. ALSBEIH, C. BADIE, EP CAPULAS, CF ARLETT and N. EP MALAISE, *Hypersensitivity of ataxia telangiectasia fibroblasts to ionizing radiation is associated with a repair deficiency of DNA double-strand breaks*. *International journal of radiation biology*, 1997. **72**(3): p. 271-283.
150. Rogakou, E.P., et al., *DNA double-stranded breaks induce histone H2AX phosphorylation on serine 139*. *Journal of biological chemistry*, 1998. **273**(10): p. 5858-5868.
151. Iliakis, G., *Radiation-induced potentially lethal damage: DNA lesions susceptible to fixation*. *International Journal of Radiation Biology*, 1988. **53**(4): p. 541-584.
152. Yang, D.-Q., et al., *Cytoplasmic ATM protein kinase: an emerging therapeutic target for diabetes, cancer and neuronal degeneration*. *Drug discovery today*, 2011. **16**(7-8): p. 332-338.
153. Lim, D.-S., et al., *ATM binds to β -adaplin in cytoplasmic vesicles*. *Proceedings of the National Academy of Sciences*, 1998. **95**(17): p. 10146-10151.
154. Varela, I., et al., *Combined treatment with statins and aminobisphosphonates extends longevity in a mouse model of human premature aging*. *Nature medicine*, 2008. **14**(7): p. 767.
155. Sera, N., et al., *The association between chronic kidney disease and cardiovascular disease risk factors in atomic bomb survivors*. *Radiation research*, 2012. **179**(1): p. 46-52.
156. Cheng, J.C., T.E. Schultheiss, and J.Y. Wong, *Impact of drug therapy, radiation dose, and dose rate on renal toxicity following bone marrow transplantation*. *International Journal of Radiation Oncology* Biology* Physics*, 2008. **71**(5): p. 1436-1443.
157. Joubert, A., et al., *DNA double-strand break repair defects in syndromes associated with acute radiation response: at least two different assays to predict intrinsic radiosensitivity?* *International journal of radiation biology*, 2008. **84**(2): p. 107-125.
158. Gomez-Munoz, A., et al., *Short-chain ceramide-1-phosphates are novel stimulators of DNA synthesis and cell division: antagonism by cell-permeable ceramides*. *Molecular Pharmacology*, 1995. **47**(5): p. 833-839.
159. Gómez-Muñoz, A., et al., *Stimulation of DNA synthesis by natural ceramide 1-phosphate*. *Biochemical Journal*, 1997. **325**(2): p. 435-440.
160. Gómez-Muñoz, A., et al., *Ceramide-1-phosphate blocks apoptosis through inhibition of acid sphingomyelinase in macrophages*. *Journal of lipid research*, 2004. **45**(1): p. 99-105.
161. Gómez-Muñoz, A., et al., *Ceramide-1-phosphate promotes cell survival through activation of the phosphatidylinositol 3-kinase/protein kinase B pathway*. *FEBS letters*, 2005. **579**(17): p. 3744-3750.
162. Hinkovska-Galcheva, V.T., et al., *The formation of ceramide-1-phosphate during neutrophil phagocytosis and its role in liposome fusion*. *Journal of Biological Chemistry*, 1998. **273**(50): p. 33203-33209.
163. Hinkovska-Galcheva, V., et al., *Ceramide 1-phosphate, a mediator of phagocytosis*. *Journal of Biological Chemistry*, 2005. **280**(28): p. 26612-26621.
164. Chalfant, C.E. and S. Spiegel, *Sphingosine 1-phosphate and ceramide 1-phosphate: expanding roles in cell signaling*. *Journal of cell science*, 2005. **118**(20): p. 4605-4612.

165. Pettus, B.J., et al., *The coordination of prostaglandin E2 production by sphingosine-1-phosphate and ceramide-1-phosphate*. *Molecular pharmacology*, 2005. **68**(2): p. 330-335.
166. Ledeen, R.W. and G. Wu, *Thematic review series: sphingolipids. Nuclear sphingolipids: metabolism and signaling*. *Journal of lipid research*, 2008. **49**(6): p. 1176-1186.
167. Alessenko, A. and S. Chatterjee, *Neutral sphingomyelinase: localization in rat liver nuclei and involvement in regeneration/proliferation*. *Molecular and cellular biochemistry*, 1995. **143**(2): p. 169-174.
168. Neitcheva, T. and D. Peeva, *Phospholipid composition, phospholipase A2 and sphingomyelinase activities in rat liver nuclear membrane and matrix*. *The international journal of biochemistry & cell biology*, 1995. **27**(10): p. 995-1001.
169. Albi, E. and M.V. Magni, *Chromatin neutral sphingomyelinase and its role in hepatic regeneration*. *Biochemical and biophysical research communications*, 1997. **236**(1): p. 29-33.
170. Albi, E. and M.V. Magni, *Sphingomyelin synthase in rat liver nuclear membrane and chromatin*. *FEBS letters*, 1999. **460**(2): p. 369-372.
171. Albi, E. and M. Viola Magni, *Sphingomyelin: a small-big molecule in the nucleus*. *Recent Res Develop Biophys Biochem*, 2006. **37**(661): p. 211-27.
172. Tomassoni, M.-L., D. Amori, and M.V. Magni, *Changes of nuclear membrane lipid composition affect RNA nucleocytoplasmic transport*. *Biochemical and biophysical research communications*, 1999. **258**(2): p. 476-481.
173. Konstantinopoulos, P.A. and A.G. Papavassiliou, *Multilevel modulation of the mevalonate and protein-prenylation circuitries as a novel strategy for anticancer therapy*. *Trends in pharmacological sciences*, 2007. **28**(1): p. 6-13.
174. Demierre, M.-F., et al., *Statins and cancer prevention*. *Nature Reviews Cancer*, 2005. **5**(12): p. 930.
175. Greenwood, J., L. Steinman, and S.S. Zamvil, *Statin therapy and autoimmune disease: from protein prenylation to immunomodulation*. *Nature Reviews Immunology*, 2006. **6**(5): p. 358.
176. Giraud, E., M. Inoue, and D. Hanahan, *An amino-bisphosphonate targets MMP-9-expressing macrophages and angiogenesis to impair cervical carcinogenesis*. *The Journal of clinical investigation*, 2004. **114**(5): p. 623-633.
177. Roelofs, A.J., et al., *Molecular mechanisms of action of bisphosphonates: current status*. *Clinical Cancer Research*, 2006. **12**(20): p. 6222s-6230s.